

**LAPORAN AKHIR PENELITIAN
PENELITIAN KOMPETITIF NASIONAL**



**EFEK JANGKA PANJANG PENGGUNAAN NANO SILIKA
TERHADAP SIFAT MEKANIK DAN DURABILITAS BETON**

TIM PENGUSUL

Peneliti Utama : DR.Ir. Jonbi, MT.,MM.,MSi
Anggota : Dr. Partogi H. Simatupang,MT

**UNIVERSITAS PANCASILA
NOVEMBER 2019**

HALAMAN PENGESAHAN

Judul : Efek Jangka Panjang Penggunaan Nano Silika Terhadap Sifat Mekanik dan Durabilitas Beton

Peneliti/Pelaksana

Nama Lengkap : Dr Ir JONBI, M.Si, M.M, M.T
Perguruan Tinggi : Universitas Pancasila
NIDN : 0301106303
Jabatan Fungsional : Lektor Kepala
Program Studi : Teknik Sipil
Nomor HP : 0816830086
Alamat surel (e-mail) : jonbi@univpancasila.ac.id

Anggota (1)

Nama Lengkap : Dr PARTOGI H SIMATUPANG S.T, M.T
NIDN : 0020017501
Perguruan Tinggi : Universitas Nusa Cendana

Institusi Mitra (jika ada)

Nama Institusi Mitra : -
Alamat : -
Penanggung Jawab : -
Tahun Pelaksanaan : Tahun ke 2 dari rencana 2 tahun
Biaya Tahun Berjalan : Rp 73,767,195
Biaya Keseluruhan : Rp 73,767,195

Mengetahui,
Dekan FTUP



Jakarta, 1 - 11 - 2019
Ketua,

(Dr Ir JONBI, M.Si, M.M, M.T)
NIP/NIK 0301106303

Menyetujui,
Ka. LPPM Universitas Pancasila



LAPORAN AKHIR PENELITIAN

1. IDENTITAS PENELITIAN (diisikan sesuai dengan proposal)

A. JUDUL PENELITIAN

EFEK JANGKA PANJANG PENGGUNAAN NANO SILIKA TERHADAP SIFAT DURABILITAS BETON
--

B. BIDANG, TEMA, TOPIK, DAN RUMPUN BIDANG ILMU

Bidang Fokus RIRN/ Bidang Unggulan Perguruan Tinggi	Tema	Topik (jika ada)	Rumpun Bidang Ilmu
Material Maju	Teknologi Pengembangan Material Fungsional	Inovasi teknologi material bahan bangunan lokal	Teknik Sipil

C. KATEGORI, SKEMA, SBK, TARGET TKT DAN LAMA PENELITIAN

Kategori (Kompetitif Nasional/ Desentralisasi / Penugasan)	Skema Penelitian	Strata (Dasar/ Terapan/ Pengembangan)	SBK (Dasar/ Terapan/ Pengembangan)	Target Akhir TKT	Lama Penelitian (Tahun)
Penelitian Kompetitif Nasional	Penelitian Dasar	SBK Riset Dasar	SBK Riset Dasar	3	2 (Dua Tahun)

2. IDENTITAS PENGUSUL

Nama, Peran	Perguruan Tinggi/ Institusi	Program Studi/ Bagian	Bidang Tugas	ID Sinta	H-Index
Dr. Ir. Jonbi, MT., MM., MSi	Universitas Pancasila	Struktur dan Material	Pengujian sampel	5996551	4
Dr. Partogi H. Simatupang, MT	Universitas Cendana	Struktur dan Material	Analisis	5982238	2

3. MITRA KERJASAMA PENELITIAN (JIKA ADA)

Mitra	Nama Mitra

4. LUARAN DAN TARGET

CAPAIAN Luaran Wajib

Tahun Luaran	Jenis Luaran	Status Target Capaian (accepted, published, terdaftar atau granted, atau status lainnya)	Keterangan (url dan nama jurnal, penerbit, url paten, keterangan sejenis lainnya)
2019	Jurnal Internasional bereputasi	Terdaftar EFFECTS OF NANO SILICA ON MECHANICAL PROPERTIES OF HIGH STRENGTH CONCRETE	KSCE Journal of Civil Engineering
2019	Jurnal Nasional terakreditasi	Terdaftar Pengembangan Paving Geopolimer Berbahan Fly Ash	Jurnal Teknik Sipil ITB Terakreditasi (S2)
2019	Prosiding Internasional terindeks	Published The long-term effects of nano-silica on concrete	doi:10.1088/1757-899X/508/1/012038
2019	Prosiding Internasional terindeks	Telah disubmit Comparative of the use of carbon and steel fiber to the mechanical properties of self compacting concrete	The 4 th International conference on functional materials and matalurgy Osaka, japan November 27-30, 2019
2019	Jurnal Nasional terakreditasi	Terdaftar Komparasi GGBFS dan FLY ASH dicampur dengan Nanaosilika terhadap sifat mekanis mortar	Jurnal Infrastruktur Universitas Pancasila Akreditasi (S3)

Luaran Tambahan

Tahun Luaran	Jenis Luaran	Status Target Capaian (accepted, published, terdaftar atau granted, atau status lainnya)	Keterangan (url dan nama jurnal, penerbit, url paten, keterangan sejenis lainnya)
2019	Paten sederhana Mesin mixer untuk mortar	<i>Terdaftar</i> <i>No.S002019908789</i>	Direktorat Jenderal Kekayaan Intelektual

2019	Buku ajar Aplikasi Nanoteknologi Pada Beton (EDISI 2)	<i>Draft</i>	Penerbit John Idetama Teknik
------	---	--------------	---------------------------------

5. KEMAJUAN PENELITIAN

Ringkasan penelitian berisi latar belakang penelitian, tujuan dan tahapan metode penelitian, luaran yang ditargetkan, serta uraian TKT penelitian yang diusulkan.

A. RINGKASAN

Penelitian penggunaan nano silika pada beton sudah banyak dilakukan peneliti. Hasilnya memperlihatkan kuat tekan dan durabilitas beton secara signifikan meningkat. Namun sayangnya penelitian yang dilakukan sebatas pada beton berumur 28 hari (jangka pendek). Sedangkan penelitian tentang efek nanosilika pada beton berumur lebih dari 28 hari (jangka panjang) masih sangat terbatas. Untuk itu perlu dilakukan penelitian efek jangka panjang penggunaan nano silika. Penelitian ini dilakukan dalam dua tahun, pada tahun pertama dilakukan pada beton f'_c 35 MPa dan f'_c 45 MPa (*moderate-high strength*). Pada tahun kedua pada beton f'_c 50 MPa dan f'_c 70 MPa (*high strength concrete*). Prosentase nano silika yang digunakan tetap sebesar 5% dari berat binder. Pengujian sifat mekanik berupa kuat tekan, kuat tarik, kuat lentur dan durabilitas beton pada umur beton 28 hari (beton kontrol), 56, 91, 365 hari. Kemudian pada setiap benda uji tersebut dilakukan pengujian SEM dan FT-IR. Hasil penelitian yang dilakukan selama dua tahun, akan dihasilkan suatu temuan baru (*novelty*) berupa nilai faktor keamanan untuk menentukan nilai mekanik dan durabilitas beton.

Hasil penelitian berisi kemajuan pelaksanaan penelitian, data yang diperoleh, dan analisis yang telah dilakukan

B. HASIL PENELITIAN

Benda uji	Pengujian pada beton umur 28, 56, 91 dan 356 hari				
	Kuat tekan	Kuat lentur	Kuat tarik	SEM	FT-IR
f'_c 50	✓	✓	✓	✓	✓
f'_c 70	✓	✓	✓	✓	✓

Status Luaran berisi status tercapainya luaran wajib yang dijanjikan dan luaran tambahan (jika ada). Uraian status luaran harus didukung dengan bukti kemajuan ketercapaian luaran dengan bukti tersebut di bagian Lampiran

C. STATUS LUARAN

Tahun Luaran	Jenis Luaran (WAJIB)	Status Target Capaian (accepted, published, terdaftar atau granted, atau status lainnya)	Keterangan (url dan nama jurnal, penerbit, url paten, keterangan sejenis lainnya)
2019	Jurnal Internasional bereputasi	Draft EFFECTS OF NANO SILICA ON MECHANICAL PROPERTIES OF HIGH STRENGTH CONCRETE	KSCE Journal of Civil Engineering
2019	Jurnal Nasional terakreditasi	Terkirim Pengembangan Paving Geopolimer Berbahan Fly Ash	Jurnal Teknik Sipil ITB Terakreditasi (S2)
2019	Prosiding Internasional	Published The long-term effects of	doi:10.1088/1757-899X/508/1/012038
2019	Prosiding Internasional terindeks	Telah disubmit Comparative of the use of carbon and steel fiber to the mechanical properties of self compacting concrete	The 4th International conference on functional materials and matalurgy Osaka, japan November 27-30, 2019
2019	Jurnal Nasional terakreditasi	Terkirim Komparasi GGBFS dan FLY ASH dicampur dengan Nanaosilika terhadap sifat mekanis mortar	Jurnal Infrastruktur Universitas Pancasila Akreditasi (S3)

Luaran Tambahan

Tahun Luaran	Jenis Luaran	Status Target Capaian (accepted, published, terdaftar atau granted, atau status lainnya)	Keterangan (url dan nama jurnal, penerbit, url paten, keterangan sejenis lainnya)
2019	Paten sederhana Mesin mixer untuk mortar	<i>Terdaftar</i> <i>No.S002019908789</i>	Direktorat Jenderal Kekayaan Intelektual
2019	Buku ajar Aplikasi Nanoteknologi Pada Beton (EDISI 2)	<i>Draft</i>	Penerbit John Idetama Teknik

Peran Mitra (untuk Penelitian Terapan, Penelitian Pengembangan, PTUPT, PDUPT serta KRUPPT) berisi uraian realisasi kerjasama dan realisasi kontribusi mitra, baik *in-kind* dan *in-cash*.

F. PERAN MITRA

Kendala Pelaksanaan Penelitian berisi kesulitan atau hambatan yang dihadapi selama melakukan penelitian dan mencapai luaran yang dijanjikan

G. KENDALA PELAKSANAAN PENELITIAN

Prosentase pencairan dana yang disetujui yang terlalu sedikit/kecil dari dana yang diajukan, cukup menyulitkan peneliti dalam pelaksanaan penelitian.

Rencana Tahapan Selanjutnya berisi tentang rencana penyelesaian penelitian dan rencana untuk mencapai luaran yang dijanjikan

H. RENCANA TAHAPAN SELANJUTNYA

- Mendaftarkan **paten Hak Cipta** untuk paper yang telah publikasi.
- Mempersiapkan publikasi paper yang akan di submit ke **KSCE Journal of Civil Engineering (impact factor: 0.600) Q3 Paper**“**EFFECTS OF NANO SILICA ON MECHANICAL PROPERTIES OF HIGH STRENGTH CONCRETE**”

Daftar Pustaka disusun dan ditulis berdasarkan sistem nomor sesuai dengan urutan pengutipan. Hanya pustaka yang disitasi pada laporan kemajuan yang dicantumkan dalam Daftar Pustaka.

I. DAFTAR PUSTAKA

1. Biricik,H.,& Sharier, N.(2014). Comparative study of the characteristic of nano silica, silica fume and Fly ash-incorporated cement mortar. *Materials Research* pp.570-582.
2. Hou, P.K., Kawashiwa,S., Wang,K.j.,Corr, D.J.,Qian,J.S., & Shah, S.P (2013), Effect of colloidal nanosilica on rheological and mechanical properties of fly ash-cement mortar. *International Journal of modern trends in engineering and Research*. pp. 207-217
3. Jalal M, Mansouri E, Sharifipour M, Pouladkhan AR.(2012) , Mechanical, rheological, durability and microstructural properties of high performance self compacting concrete containing SiO₂ micro and nanoparticles. *Material Des* 34:389–400
4. Jonbi, Binsar Hariandja, Iswandi Imran, dan Ivindra Pane, (2012), The used of Nanosilica for Improving of concrete Compressive strength and Durability, *Applied Mechanics and Materials*, Vols.204-208, pp. 4059-4062.

5. Kong D, Du X, Sun W, Zhang H, Yang Y, Shah SP. (2013) Influence of nano-silica Agglomeration on microstructure and properties of the hardened cement based materials. *Construction Building Materials* 37:707–15.
6. Mohammad Bolhassani and Mohammadreza Samani (2015), Effect of type, size and Dosage of Nanosilica and Microsilica on Properties of Cement Paste and Mortar, *ACI Materials Journal* No. 112-M27 pp 259-265.
7. Mohamed Fattouh Abd El Hameed, Mariam Farouk Ghazy, and Metwally Abd Allah Abd Ela, (2016), Cement Mortar with Nanosilica: Experiments with Mixture Design Method , *ACI Materials Journal*, V. 113, No. 1, pp 43-59.
8. Oertel T, Hutter F, Tänzer R, Helbig U, SEXTL G. (2013) , Primary particle size and agglomerate size effects of amorphous silica in ultra-high performance concrete. *Cement Concrete Composites* 37:61–7.
9. Schmidt M, Amrhein K, Braun T, Glotzbach C, Kamaruddin S, Tänzer R.(2013) Nanotechnological improvement of structural materials – impact on material performance and structural design. *Cement Concrete Composites* 2013;36:3–7.
10. Sing,L.P., Goel, A., Kumar Bhattacharyya, S., Ahalawat,S.,Sharma,U.,& Mishra,G,(2015), Effect of Morphologi and dispersibility of silica nanoparticles on the Mechanical Behavior of cement mortar *International Journal of concrete structures and materials*, pp. 2017-217
11. Torabian Isfahani, F.,Redaelli,E.,Lollini,F., Li, W.,& Bertolini, L.,(2016), Effect of Nanosilica on Compressive Strength and Durability properties of Concrete with Different water to Binder Ratios, *Advances in Materials Sciences and engineering* pp.1-16.
12. Y. Al-Najjar, S. Yesilmen, A. Majeed Al-Dahawi, M. Şahmaran, G. Yıldırım, M. Lachemi, and L. Am (2016), Physical and Chemical Action of Nano-Mineral additives on properties of high-Volume fly ash *Engineering Cementitious Composites*, *ACI Materials Journal*, V. 113, No. 6. pp 791-801

Lampiran berisi bukti pendukung luaran wajib dan luaran tambahan (jika ada) sesuai dengan target capaian yang dijanjikan

J. LAMPIRAN Terlampir

Comparative of the use of Carbon and Steel Fiber to the Mechanical Properties of self Compacting Concrete

Jonbi^{1, a *}, Resti Nur Arini^{2, b}, Marisa Permatasari^{3, c}, Partogi H Simatupang^{4, d}

^{1,2,3}Civil Engineering Department, Faculty of Engineering, Pancasila University, Jakarta, Indonesia

⁴Civil Engineering Department, Faculty of Science and Engineering, University of Nusa Cendana, Kupang, Indonesia

^ananobjg@gmail.com, ^bresti.nurarini@univpancasila.ac.id, ^cpermatasari563@gmail.com

^dpartogihsimatupang@gmail.com

Keywords: Carbon fiber, steel fiber, self compacting concrete, tensile strength, flexural strength.

Abstract. This research is a comparative study, the use of carbon fiber and steel fiber for Self Compacting Concrete (SCC). In previous studies, it was proven that the addition of steel fibers can increase the compressive and tensile strength of SCC. While carbon fiber is one of the most widely used materials for structural reinforcement in recent years. Therefore it is necessary to do a comparative study of the use of carbon fiber if applied to SCC. The percentage increase in carbon fiber and steel is 0.5%, 1%, and 1.5%. Then do the testing of: slump test, compressive strength, tensile strength and flexural strength. The results showed the optimal percentage of steel fiber addition of 1.5%, can increase the compressive strength of SCC by 11%. However carbon fiber and steel do not increase the tensile strength of SCC, and tend to reduce flexural strength. Other results show that carbon fiber is not suitable for use in SCC.

Introduction

The progress of self-compacting concrete (SCC) technology is very helpful and beneficial for large volumes and very tight reinforcement distances. Some of its advantages include increased work productivity, reduced labor force, and elimination of vibrators [1-3]. However, there is continuous research on its developed, one of which is the addition of fiber to improve the mechanical properties of concrete [4]

However, this is likely to affect the workability of concrete because it has a higher specific surface compared to aggregates with the same volume. In addition, its use in a concrete mixture reduces workability depending on the type and content of the fiber utilized [5]. Addition of fiber in the concrete mixture increases compressive and tensile strength, thereby, making it more durable.

Previous research on the effect of adding 2% of steel fiber to the SCC mixture led to an increase in the tensile strength by 28.5%, with reduced workability [6]. Addition of steel fibers inhibits and increase the resistance of the concrete to cracking [7,8,9].

Carbon Reinforced Polymer (CFRP) has the advantage of having higher strength, a low weight, high stiffness, corrosion resistance, lower maintenance costs and faster installation time [10]

SCC Mix Design refers to previous studies [11]. However, modifications were made with the addition of a water volume of 4.9% and PCE type super plasticizer of 3.1%, which is capable of increasing concrete compressive strength by 26.77% [12].

This research therefore is a comparison of the use of steel and carbon fiber to the mechanical properties of SCC. It furthermore aims at producing the optimal percentage of fiber addition to improve the performance of SCC.

Methodology

Material OPC (Ordinary Portland Cement), coarse aggregate (10-20) mm and fine aggregate, type F fly ash from PT. Adhimix. In Table 1 shows the results of fine aggregate testing for Silica fume and Polycarboxylate Ether Superplasticizer (PCE).

Table 1 Fine aggregate test results

Test type	Result	Tolerance	Standard
Material Pass the Sieve No. 200 (%)	1,70	maximum of 3%	ASTM C. 117-95
Specific Gravity SSD	2,60	Minimal 2,55	ASTM C. 128-93
Absorption (%)	1,83	Maksimal 4%	ASTM C. 128-93
Fine Modulus	2,58	2,3 – 3,1	ASTM C. 33
Fill Weight	1,487	Minimal 1,2	ASTM C. 29-97
Organic Content	3	maximum 3	ASTM C. 40-92

The SCC mix design is shown in Table 2, with the proportion of specimens mix design in 1m³. The C specimen is referenced by SCC concrete (without fiber), while the C1, C2, and C3 carbon fibers have an additional 0.5%, 1%, 1.5%.

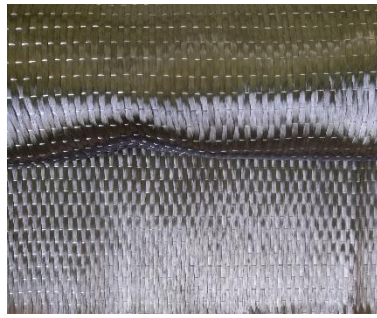
Table 2. The proportion of specimens mix design

Material	Unit	C	C1	C2	C3	S1	S2	S3
OPC	kg	400	400	400	400	400	400	400
Silica Fume	kg	50	50	50	50	50	50	50
Carbon fiber	kg	0	2,25	4,5	6,75	0	0	0
Steel fiber	kg	0	0	0	0	2,25	4,5	6,75
Coarse Aggregate	kg	657	657	657	657	657	657	657
Fine Aggregate	kg	904	904	904	904	904	904	904
Fly ash	kg	250	250	250	250	250	250	250
PCE	kg	26,5	26,5	26,5	26,5	26,5	26,5	26,5
Water	Liter	233,5	233,5	233,5	233,5	233,5	233,5	233,5

The carbon fiber used in this study is from PT. Fosroc Indonesia with brand of FRC 300, while the Steel fiber was from Dramix D. The technical data of both fibers is shown in Table 3 and Figure 1. Show carbon and steel fiber.

Table 3: Technical data on carbon fiber and steel

Grade	Carbon Fiber (FRC 300)	Steel Fiber (Dramix 3 D)
Weight	300 (g/m ²)	4.584 fibres/kg
Thickness	0.167 (mm)	Length :60 mm Diameter 0,75 mm
Tensile Strength (MPa)	3841	1225
Tensile Modulus(GPa)	230	210



Carbon fiber



Steel fiber

Fig. 1 Carbon fiber and steel fiber

Tests were carried out to determine the slump value in concrete meets the test requirements of SCC, where the slump flow test requirements are 65-85 cm and t_{50} at 2-5 seconds [13].

The compressive strength of 3.7, was obtained in 28 days using ASTM C 39/C 39M-01, while, the tensile strength of the same values were also acquired using ASTM C 496-96. Flexural testing by ASTM C78 / C78-18 resulted in a beam specimen of 150 mm x 150 mm x 600 mm, tested at 28 days.

The tests performed are shown in Figure 3. Reference and fibrous SCC concrete were carried out by slump flow test and t_{50}

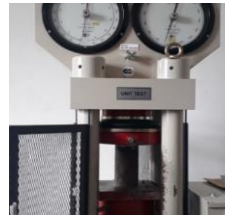


Fig.2 Testing carried out on the sample

Result and Discussions

Slump test results as shown in Table 4. Based on the test results, it turns out that the reference SCC concrete (C), the percentage of carbon fiber 0.5% (C1), 1% (C2), percentage of steel fiber 0.5% (S1), 1% (S2) and 1.5% (S3) steel, meet the requirements as SCC concrete. While Carbon fiber with a percentage of 1.5% produces slump below the standard, this is due to clumping of carbon fiber so that it does not meet existing requirements. So for the next sample addition of carbon fiber C3 no further testing of the mechanical properties (compressive strength, tensile and flexural)

Tabel 4. Slump value

Code	t ₅₀ (detik)	Standart 50 (detik)	Slump Value (cm)	Standart SCC (cm)
C	5		67	
C1	5		74	
C2	5		71	
C3	-	2 - 5	-	65 - 85
S1	4		73	
S2	4		75	
S3	4		78	

The compressive strength test results are seen in Figure 3. At 3 to 7 days, fibrous concrete increased the compressive strength, without changing its value. However, on the 28 day, the control and fibrous concrete (carbon fiber and steel fiber) increased, with the value of compressive strength C, C1, C2, C3, S1, S2, and S3 equals 40.11 MPa, 28.41 MPa, 14.83 MPa, 36.92 MPa, 39.79 MPa, and 44.56 MPa respectively.

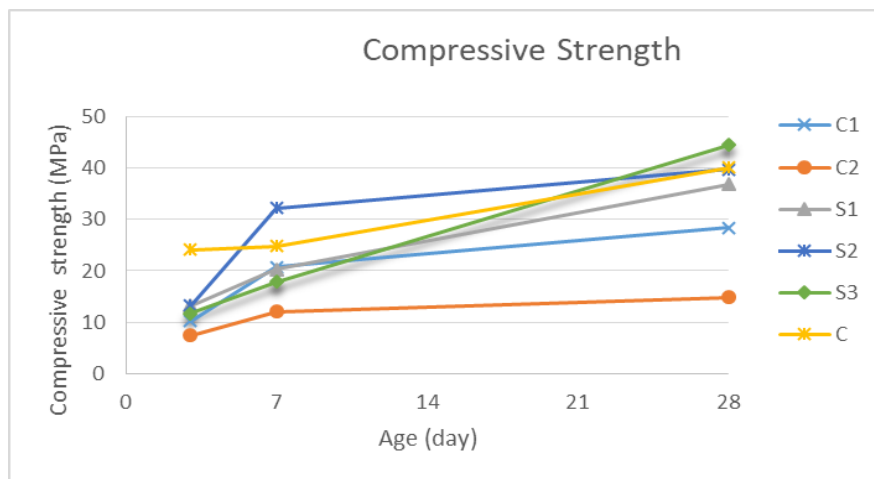


Fig.3 Result of testing the Compressive Strength

The results of this test indicate that the use of carbon fiber with high tensile strength and modulus of elasticity which is incompatible when used as an additive in SCC. The percentage of carbon fiber addition resulted in a decrease in compressive strength compared to the reference concrete. This is due to carbon fiber clumping during mixing, thereby, disrupting its homogeneity. Whereas in steel fibers, its addition percentage tends to increase the compressive strength, with an optimum percentage of 1.5%, which is in line with previous studies [14].

The tensile test results are shown in Figure 4. At 28 days the strength of carbon and steel namely C, C1, C2, S1, S2, and S3 were 3.98 MPa, 3.92 MPa, 1.99 MPa, 3.4 MPa, 3, 4 MPa, 3.45 MPa and 3.98 MPa respectively. The result of tensile strength with the percentage of steel fiber addition has a tensile strength close to the reference SCC, this is because of the adhesive between the concrete and steel fibers. While the percentage of carbon fiber addition shows a decrease in tensile strength.

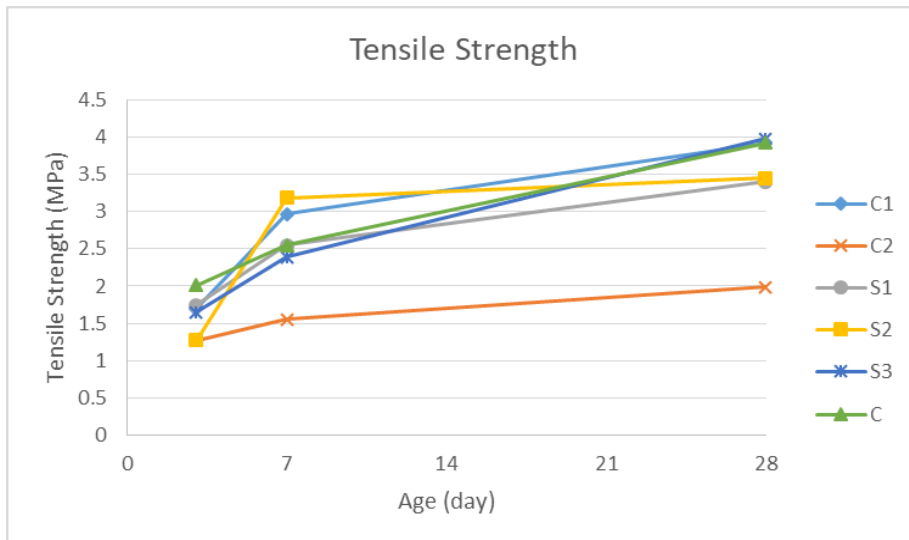


Fig.4 Result of testing the Tensile Strength

The results of the flexural strength test shown in Figure 5, indicates the value between 7 and 28 days with values of 3.05 MPa and 4.94 MPa. In fibrous concrete (carbon and steel fibers), C1, C2, S1, S2, and S3 have flexural strength values of 3.30 MPa, 2.39 MPa, 3.72 MPa, 3.50 MPa, and 3.67 MPa respectively, where the flexural strength value increased but not significant. These results are in line with previous researches [15].

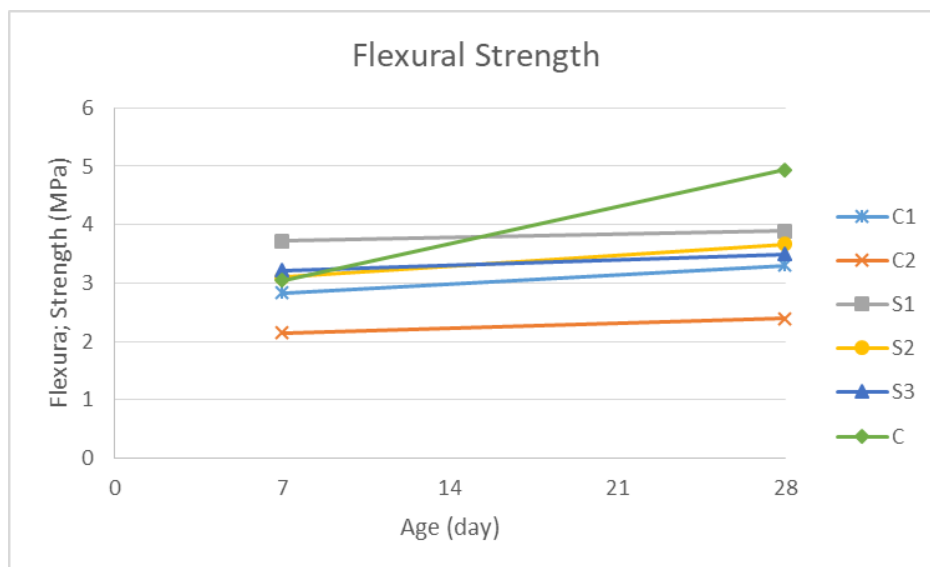


Fig.5 Result of testing the Flexural Strength

Summary

Based on the results of this experimental study, the following summary were drawn:

1. Addition of 1.5% optimum steel fiber is capable of increasing the compressive strength by 11% of the reference concrete.
2. Carbon and steel fibers do not significantly increase the tensile strength of SCC and tend to reduce its flexural strength
3. Carbon fiber is not suitable for use in SCC.

The author thanks the financial support from Ministry of Research Technology and Higher Education of the Republic of Indonesia for this Research Grant with the Scheme of Competency Based Research for the year 2019.

References

- [1] Najim, K. B. & Hall, M. R., Mechanical and dynamic properties of self-compacting crumb rubber modified concrete, *Construction and Building Materials* 27 (2012), pp. 521-530.
- [2] Jalal, M., Mansouri, E., Sharifipour, M. & Pouladkhan, A. R. Mechanical, rheological durability and microstructural properties of high performance self-compacting concrete containing SiO₂ micro and nanoparticles, *Material and Design* 34(2012) pp. 389-400.
- [3] Khalid B Najim, M. R. H., Mechanical and dynamic properties of self-compacting crumb rubber modified concrete. *Construction and Building Materials* 27 (2012), pp. 521-530.
- [4] Akcay, B. & Tasdemir, M. A., Mechanical behaviour and fibre dispersion of hybrid steel fibre reinforced self-compacting concrete, *Construction and Building Materials* 28 (2012), pp. 287-293
- [5] Grunewald, S. & Walraven, J. C. Parameter-study on the influence of steel fibers and coarse aggregates on the fresh properties of self-compacting concrete, *Cement and Concrete* 31(2001) pp. 1793-1798.
- [6] Khaloo, A., Raisi, E. M., Hosseini, P. & Tahsiri, H.,:Mechanical performance of self-compacting concrete reinforced with steel fibers, *Construction and Building Materials* 51, (2014) pp. 179-186.
- [7] Cao, Q.; Cheng, Y.; Cao, M.; and Gao, Q., Workability, Strength, and Shrinkage of Fiber Reinforced Expansive Self-Consolidating Concrete, *Construction and Building Materials*, V. 131, (2016),pp. 178-185.
- [8] Jiang, J. Y.; Sun, W.; Zhang, Y. S.; Qin, H.; and Wang, J, Research on Cracking Resistance Performance of Super Vertical-Distance Pumped Steel Fiber Concrete,*Journal of Southeast University*, V. 37 (2007), No. 1, pp. 123-127.
- [9] Qi Cao, Quanqing Gao, Jinqing Jia, and Rongxiong Gao, Early-Age Cracking Resistance of Fiber-Reinforced Expansive Self-Consolidating Concrete, *ACI Materials Journal*,V.116 (2019) No. 1
- [10] ACI 440.2R-08, Guide for Design and Construction of externally Bonded FRP system for Strengthening concrete structures, American Concrete Institute,USA,2002.
- [11] Mandandoust, R., Ranjbar, M. & Moshiri, A, The Effects of steel and PET fibers on teh properties of fresh and hardened self compacting concrete. *Construction and Building Materials* 15(2014)
- [12] Jonbi, J., Arini, R. N., Anwar, B. & Fulazzaky, M. A. Effect of added the Polycarboxylate ether on slump retention and compressive strength of the high-performance concrete. *MATEC*, Volume 195 (2018)
- [13] EFNARC : specification and guidelines for self-compacting concrete; European Federation for Specialist Construction Chemicals and Concrete Systems (2002).
- [14] El-Dieb A.S, Mechanical, durability and microstructural characteristics of ultra-highstrength self-compacting concrete incorporating Steel fiber, *Materials and Design*, **30** (2009) 4286–4292.
- [15] Soutsos, M., Le, T. & Lamporopoulos, A., Flexural Performance of Fibre Reinforced Concrete Made with Steel and Synthetic Fibres. *Construction and building materials* Volume 36 (2012) pp. 704-710.

Pengembangan Paving Geopolimer Berbahan Fly Ash

Jonbi

Prodi Teknik Sipil Fakultas Teknik Universitas Pancasila, E-mail: jonbi@univpancasila.ac.id

Partogi H.Simatupang

Prodi Teknik Sipil Fakultas Sains dan Teknik Universitas Nusa Cendana, Kupang, Provinsi NTT,
E-mail: partogihsimatupang@gmail.com

Detia Farah Ghina

Prodi Teknik Sipil Fakultas Teknik Universitas Pancasila, E-mail: detiafarahghina@gmail.com

Abstrak

Trend penelitian saat ini, lebih fokus pada bagaimana mengurangi penggunaan semen dan mengatasi masalah limbah industri salah satunya fly ash. Upaya yang dilakukann yakni mengembangkan geopolimer dengan fly ash sebagai bahan utama, dan menggunakan Natrium Hidroksida (NaOH) dan Sodium Silicate (Na_2SiO_3) sebagai activator. Tujuan dari penelitian ini adalah menghasilkan rasio NaOH : Na_2SiO_3 yang paling optimum dan menghasilkan paving block yang sesuai standar SNI. Dalam penelitian ini rasio activator NaOH : Na_2SiO_3 yang digunakan sebesar 1: 0,5 ; 1:1 ; 1:1,5 ; 1:2 dengan konsentrasi molaritas 11 M. Kemudian dibuat sampel uji berupa paving block dengan ukuran (200 x 110 x 80). Pengujian dilakukan kuat tekan pada umur ke 7, 14, dan 28 hari dan uji penyerapan air pada umur 28 hari. Hasil penelitian memperlihatkan rasio optimum activator adalah 1:2, menghasilkan paving block dengan kuat tekan dan workability yang tinggi. Kemudian rasio 1:1 ; 1:1,5 ; 1:2 memiliki kuat lebih dari 17 MPa termasuk mutu B dapat digunakan untuk area parkir. sedangkan rasio 1:0,5, menghasilkan paving mutu C dapat digunakan untuk pejalan kaki. Perbandingan harga paving geopolimer tersebut dengan harga paving berbahan semen yang beredar di pasaran juga turut dipresentasikan. Benefit dari penelitian ini, dapat menjadi salah satu solusi untuk mengatasi isu pencemaran lingkungan dan limbah industri..

Kata-kata Kunci: Paving Geopolimer, Fly Ash, Kuat Tekan, Penyerapan air.

Abstract

Current research trends are focused on reducing the use of cement and managing industrial waste, including fly ash, which is handled through its proper use as the main ingredient in geopolymers, along with Sodium Hydroxide (NaOH) and Sodium Silicate (Na_2SiO_3) as activators. This study, therefore, aims to produce the most optimal NaOH activator: Na_2SiO_3 ratio required in the production of concrete Paving block under the SNI standards, and those evaluated in this study include 1:0.5, 1:1, 1:1.5, and 1:2 with 11 molarity concentrations. In addition, the samples investigated were 200 x 110 x 80 cm concrete paving block, and compressive strength testing was performed on day 7, 14, and 28, while water absorption was assessed on a 28-day. The results showed 1:2 to be the optimal ratio, based on the high compressive strength and the superior workability of its concrete paving block. Furthermore, it was established that the activator ratios of 1:1, 1:1.5, 1:2 produced B-quality concrete paving block, with a compressive strength of 17 MPa, with possible application in a parking area. Also, the 1:0.5 preparations were of C quality with the probability of being used on the sidewalk. The comparison of the price of geopolymer paving and cement based paving is also presented. Thus, the study outcomes were candidates for adoption in the quest to overcome environmental pollution and industrial waste.

Keywords: Geopolymer Paving, Fly Ash, Compressive Strength, Water absorption.

1. Pendahuluan

Penggunaan semen sebagai pengikat pada campuran beton dan mortar berdampak negatif terhadap lingkungan. Data menunjukkan sebanyak 7% gas CO_2 yang ada di atmosfer berasal dari industri semen, karena memproduksi 1 ton semen akan menghasilkan 1 ton gas CO_2 ke dalam atmosfer dan menjadi salah satu pemicu pemanasan global [1,2]. Kemudian limbah dari PLTU berupa fly ash dan bottom ash yang berpotensi mencemari lingkungan dan termasuk limbah B3.

Berbagai penelitian inovasi telah dilakukan untuk mengurangi penggunaan semen atau tanpa menggunakan semen sama sekali dikenal sebagai geopolimer. Hasil penelitian menunjukkan bahwa geopolimer dapat menjadi salah satu solusi mengatasi limbah logam berat yang berbahaya dari industri modern dan dapat digunakan sebagai bahan pengganti semen [3,4].

Salah satu pemanfaatan perkembangan geopolimer dalam mengatasi masalah limbah Fly ash yakni dengan dijadikan sebagai paving block. Hal ini seiring dengan meningkatnya kebutuhan terhadap paving block karena memiliki beberapa keuntungan antara lain: ramah lingkungan dan sangat baik dalam membantu konsevasi air tanah, mudah dan cepat dalam pemasangan. Menurut peneliti lain Kemudian peneliti lain menyatakan bata

geopolimer dapat mengurangi emisi CO₂ hingga 59 % dibandingkan pembuatn batu bata dengan proses pembakaran [5].

Fly ash sangat potensial untuk dimanfaatkan sebagai bahan campuran paving block geopolimer karena mengandung nilai silica dan alumunia yang tinggi. Fly Ash yang digunakan diaktifkan dengan larutan alkali berupa Sodium Hidroksida (NaOH) dan Sodium Silikat (Na₂SiO₃) sebagai katalisatornya. Campuran aktivator NaOH dan Sodium silikat pada geopolimer lebih mudah dibuat dan ramah lingkungan dalam hal toksisitas dan leaching [6-13].

Larutan alkali tinggi digunakan untuk mengaktifkan fly ash untuk membentuk pasta yang mengikat aggerat kasar dan agregat halus dan bahan tidak bereaksi lainnya dicampurkan. Hasil penelitian mengungkapkan bahwa heatcured pada Geopolimer akan menghasilkan kuat tekan yang relatif tinggi, susut rendah, dan ketahanan yang baik terhadap sulfat dan asam [8].

Proses pembuatan paving block geopolimer dengan bahan fly ash diharapkan dapat mengurangi emisi CO₂ dan mengurangi limbah B3 fly ash. Saat ini kebutuhan paving block pada industri pekerasan area parkir mobil (mutu B) meningkat tinggi.

Tujuan dari penelitian ini adalah menentukan komposisi optimum variasi rasio Na₂SiO₃ yang menghasilkan kuat tekan dan workability tinggi. Penelitian paving block geopolimer meliputi pengujian sifat mekanik yakni kuat tekan BS 6717-1-1993, dengan persyaratan kuat tekan minimum 17 MPa untuk kategori paving block mutu B yang dapat di aplikasikan untuk area parkir mobil. Sedangkan mutu C, kuat tekan minimum 12.5 MPa untuk area pejalan kaki.[9]. Sedangkan persyaratan penyerapan air menurut SNI 03-0691-1996 untuk mutu B air rata-rata maksimum 6% , dan untuk mutu C sebesar 8% [10].

Benefit penelitian ini dapat menjadi salah satu alternatif mengatasi masalah semen dan fly ash menjadi material konstruksi berupa paving block geopolimer.

2. Material

Material yang digunakan pada penelitian ini adalah agregat kasar (kerikil) maksimum berukuran diameter 1 cm, agregat halus (pasir) dan fly ash tipe C berasal dari PT. Adhimix Precast Indonesia, Air berasal dari laboratorium PT. Adhimix Precast Indonesia, Alkali aktivator yang digunakan adalah Serpihan Natrium Hidroksida (NaOH) dan Larutan Sodium Silikat (Na₂SiO₃), pada Gambar 1.



Gambar 1. Material yang digunakan dalam penelitian

3. Metode Penelitian

Penelitian ini dilakukan dengan tahapan sebagai berikut: persiapan bahan baku, trial mix, membuat rancang campur paving block geopolimer, pembuatan benda uji, pengujian benda uji (uji kuat tekan dan penyerapan air), dan analisis hasil pengujian. Pembuatan benda uji paving block geopolimer dengan aktivator gabungan larutan NaOH dan Na₂SiO₃. Variasi rasio NaOH : Na₂SiO₃ sebesar 1:0,5 ; 1:1 ; 1:1,5 ; 1:2 dengan konsentrasi NaOH sebesar 11 M.

Berdasarkan pembuatan larutan yang telah dilakukan sebelumnya bahwa untuk pembuatan NaOH 11 M dapat secara praktis dilakukan dengan melarutkan 440 gram kepingan NaOH dengan 800 ml air suling (800 gram). Kemudian larutan NaOH 11 M dengan volume 1 liter tersebut didiamkan selama ± 24 jam, lalu direaksikan dengan Na₂SiO₃ sesuai dengan takaran per perbandingan seperti terlihat pada Gambar 2.

Pencampuran antara air dan serpihan NaOH harus dilakukan pada wadah tertutup dan di diamkan ± 6 jam, karena terjadi peningkatan suhu hingga 110° C. Fungsi dari di tutupnya wadah berisikan air dan serpihan NaOH atau yang di sebut alkali aktivator adalah menurunkan suhu campuran hingga 24°-27° C. Setelah itu larutan alkali activator di campurkan dengan Na₂SiO₃ yang berfungsi memperkuat ikatan polimerisasi. Pencampuran ini dapat meningkatkan suhu campuran hingga 40°, sehingga campuran harus di diamkan ± 6 jam dengan wadah tertutup. Hal ini berfungsi agar larutan activator yang nantinya akan dicampurkan dengan fly ash tidak terjadi gumpalan, dan dapat menyebabkan kegagalan dalam proses polimerisasi.



Gambar 2. Proses pembuatan larutan aktivator

Pada Tabel 1 terlihat proporsi campuran paving block geopolimer dengan variasi rasio activator.

Tabel 1. Proporsi campuran Paving Block Geopolimer

Fly Ash	Agregat		NaOH (M)	Variasi	Aktivator /FA
	Kasar	Halus			
1	1,36	2,53	11	1:0,5	0.37
1	1,36	2,53	11	1:1	0.32
1	1,36	2,53	11	1:1,5	0.28
1	1,36	2,53	11	1:2	0.25

Sedangkan untuk variasi rasio aktivator dan jumlah sampel paving block berukuran 200 x 110 x 80 mm dapat dilihat pada Tabel 2.

Tabel 2. Variasi rasio aktivator dan jumlah sample paving block

Variasi rasio Aktivator	Jumlah sampel (Buah)	Jumlah sampel berdasarkan Umur (Hari)		
		7	14	28
1:0,5	18	6	6	6
1:1	18	6	6	6
1:1,5	18	6	6	6
1:2	18	6	6	6

Pengujian yang dilakukan adalah pengujian kuat tekan pada umur 7, 14 dan 28 hari. Pengujian penyerapan air dengan cara perendaman juga dilakukan untuk paving yang berumur 28 hari. Pengujian yang dilakukan dalam penelitian ini diberikan pada Gambar 3 dan Gambar 4 berikut.



Gambar 3. Pengujian kuat tekan paving geopolimer



Gambar 4. Pengujian penyerapan air paving geopolimer

4. Hasil dan Pembahasan

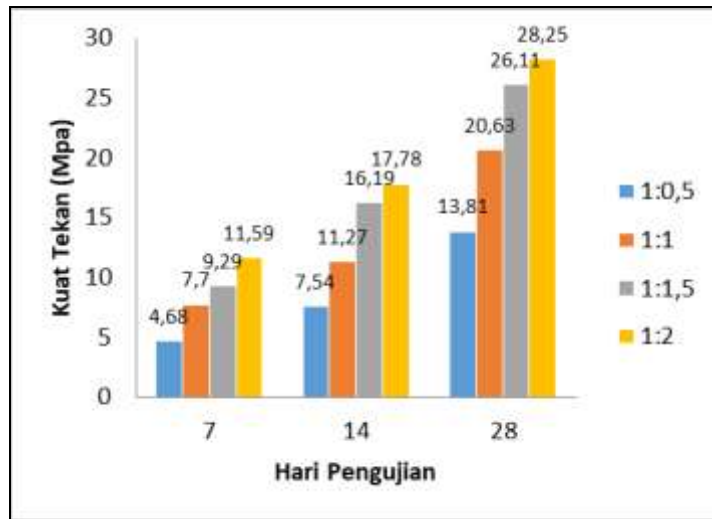
Paving geopolimer yang dihasilkan pada penelitian ini memiliki bentuk dan penampilan yang hampir sama dengan paving berbahan semen. Semakin banyak larutan natrium silikat (Na_2SiO_3) yang diberikan semakin baik dan halus permukaan paving yang dihasilkan. Berbagai produk paving geopolimer penelitian ini ditampilkan pada Gambar 5 berikut.



Gambar 5. Produk paving geopolimer yang dihasilkan

Pada Gambar 6. memperlihatkan hasil pengujian kuat tekan paving block geopolimer, nilai kuat tekan tertinggi pada umur 28 hari yaitu pada rasio 1:2 sebesar 28,25 MPa, dan nilai kuat tekan terendah pada rasio 1:0,5 yaitu 11,59 MPa. Peningkatan penambahan rasio 1:0,5 sampai 1:1 kuat tekan mengalami peningkatan masing-masing sebesar 6,82 MPa atau sebesar 33.06%, pada variasi 1:1 sampai 1:1,5 mengalami kenaikan sebesar 5,48 MPa atau sebesar 20.98% kemudian pada variasi 1:1,5 sampai 1:2 mengalami kenaikan kembali sebesar 2,14 MPa atau sebesar 7,57%. Hal ini menunjukkan penambahan rasio $\text{NaOH}:\text{Na}_2\text{SiO}_3$ dapat meningkatkan kuat tekan hal ini sejalan dengan penelitian sebelumnya [11,12].

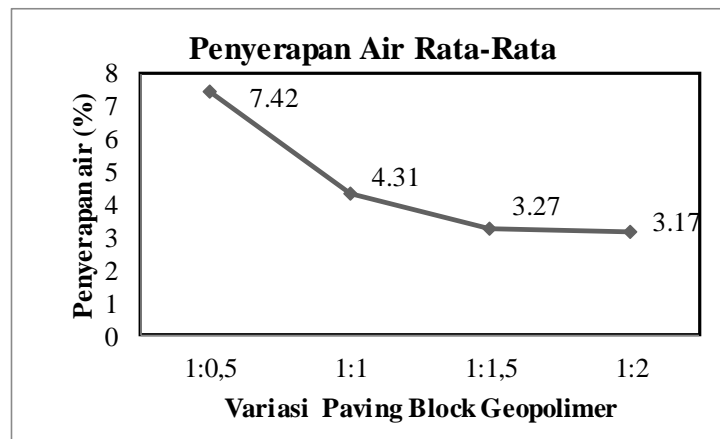
Hasil ini memperlihatkan paving block rasio activator sebesar 1:1 , 1:1,5 ,1:2 memenuhi persyaratan sebagai mutu B dapat diaplikasi pada area parkir. Sedangkan rasio activator untuk kategori mutu C untuk area pejalan kaki.



Gambar 6. Hubungan Umur Pengujian Terhadap Kuat Tekan Paving Block Geopolimer

Pada Gambar 7. memperlihatkan hasil uji penyerapan air, dengan rasio 1:0,5 menghasilkan penyerapan air tertinggi 7.42% dan rasio 1:2 terendah sebesar 3.17%. Peningkatan rasio Na_2SiO_3 akan menurunkan persentase penyerapan air. Dengan demikian rasio sebesar 1:0,5 1:2 rata-rata penyerapan air mengalami penurunan sebesar 41.90%, 24.12%, dan 3.06%.

Penyerapan air paving block dengan rasio 1:1, 1:1,5 dan 1:2 memiliki penyerapan air < 6 % mutu B yang dapat digunakan pada area parkir mobil. Sedangkan untuk rasio 1: 0.5 memiliki nilai penyerapan 7.42 % < 8% mutu C digunakan untuk area pejalan kaki.



Gambar 7. Hasil uji penyerapan air rata-rata paving block geopolimer

Perbandingan harga dilakukan dengan melakukan analisa harga paving geopolimer diberikan pada Tabel 3. Adapun campuran yang diambil adalah campuran 1:0.5 yang menghasilkan harga termurah.

Harga paving geopolimer dalam penelitian ini memiliki nilai paling murah sebesar Rp. 8.410,- per buah. Sementara harga paving block berbahan semen dipasaran yaitu berkisar Rp.2.500, per buah. Hal ini menunjukkan harga paving block geopolimer lebih mahal berkisar 3 s/d 4 kali harga paving block berbahan semen yang ada dipasaran. Komponen paling mahal dalam pembentuk harga paving geopolimer adalah harga larutan activator baik itu larutan natrium silikat maupun natrium hidroksida padat. Harga paving block geopolimer akan kompetitif dengan harga paving block yang ada dipasaran jika harga larutan activator tersebut dapat ditekan sekecil mungkin

Tabel 3. Analisa harga per unit paving block geopolimer

No.	Bahan	Volume	Satuan	Harga Satuan	Biaya
1	Fly Ash	0.56	kg	-	-
2	NaOH solid	0.11	kg	10.000	1.100
3	Air Suling	0.2	kg	1.000	200
4	Sodium Silikat (Na ₂ SiO ₃)	0.06	kg	10.000	600
5	Kerikil	0.76	kg	3.000	2.280
6	Agregat Halus	1.41	kg	3.000	4.230
TOTAL HARGA PER UNIT					8.410

5. Kesimpulan dan Saran

Komposisi optimum rasio aktivator NaOH : Na₂SiO₃ sebesar : 1: 2 yang menghasilkan kuat tekan dan workability tinggi. Paving Block yang dihasilkan pada rasio aktivator 1:1, 1:1,5 1:2 dapat digunakan untuk area parkir mobil (Mutu B). Paving Block dengan rasio aktivator sebesar 1: 0,5 dapat digunakan untuk pejalan kaki (mutu C).

Biaya paving block geopolimer belum kompetitif dibandingkan dengan harga paving berbahan semen yang ada dipasaran sekarang ini karena harga paving geopolimer masih sangat mahal yaitu berkisar 3 s/d 4 kali dibandingkan harga paving berbahan semen. Biaya larutan activator harus dapat ditekan sekecil mungkin agar dapat menghasilkan harga paving geopolimer yang kompetitif.

6. Daftar Pustaka

- A. Muthadi and V. Dhivya. Investigating Strength Properties of geopolimer Concrete with Quarry Dust. *ACI material journal*, V. 114. No.3. 2017. pp 355-363
- Al-Majidi, M. H., Lampropoulos, A., Cundy, A., and Meikle, S. Development of geopolimer mortar under ambient temperature for in situ applications. *Construction and Building Materials*, 2016, 120, pp.198-211
- BS 6717-1:1993, Precast concrete paving blocks. Specification for paving blocks
- Guo X, Hu W, Shi H. Microstructure and self solidification/stabilization (S/S) of Heavy metal of nano modified CFA-MSWIPA composite geopolymers *Constr. Build. Mater*, 2014 **56**, 81-86
- Hardjito, D.; Wallah, S. E.; Sumajouw, D. M. J.; and Rangan, B. V., "On the Development of Fly Ash-Based Geopolymer Concrete," *ACI Materials Journal*, V. 101, No. 6, Nov.-Dec. 2004, pp. 467-472
- Kumar, A. and Kumar, S. Development of paving blocks from synergistic use of red mud and fly ash using geopolymerization. *Construction and Building Materials*, 2013 38, pp.865-871
- Mali Basil, Study on Geopolymer concrete used for paving block, Department of Civil Engineering M G University, India, 2016
- Nguyen Van Chanh., Bui Dang Trung. Recent Reasearch in Geopolymer Concrete, 3nd ACF Internasional Conference. 2008, pp. 235-241
- Nicolas Youssef, Andry Zaid Rabenantoandro, Zakaria Dakhli, Fadi Hage Chehade, and Zoubeir Lafhaj. "Enviromental Evaluation of Geopolymer Bricks". *MATEC Web of Conferences* , France. INCER. 2019
- Simatupang, P.H., Imran, I., Pane, I., and Sunendar, B., On the Development of a Nomogram for Alkali Activated Fly Ash Material (AFAM) Mixtures . *J.Eng.Technol.Sci*, 2015, Vol 47.No.3, pp.231-249

Standar Nasional Indonesia untuk Paving Block. SNI-03-06910-1996. 1996. Bata Beton (paving block)

Temuujin, J; Van Riessen, A.; and William, R., "Influence of Calcium Compounds on the Mechanical Properties of Fly-Ash Geopolymer Concrete". *Journal of Materials in Civil Engineering, ASCE*, V. 27, No. 7, 2015, pp. 1-7. doi: 10.1061/(ASCE)MT.1943-5533.0001157

V. Bhiksha, M. Koti Reddy and t. Srinivas Rao. An Experimental Investigation On Properties Of Geopolymer Concrete (No Cement Concrete). *Asian Journal Of Civil Engineering, India* 2011. pp 842-853

PAPER • OPEN ACCESS

The long-term effects of nano-silica on concrete

To cite this article: Jonbi *et al* 2019 *IOP Conf. Ser.: Mater. Sci. Eng.* **508** 012038

View the [article online](#) for updates and enhancements.



IOP | ebooks™

Bringing you innovative digital publishing with leading voices to create your essential collection of books in STEM research.

Start exploring the collection - download the first chapter of every title for free.

The long-term effects of nano-silica on concrete

Jonbi^{1*}, P H Simatupang², A Andreas¹ and A Nugraha¹

¹ Civil Engineering Department, Faculty of Engineering, University of Pancasila, Jakarta, Indonesia

² Civil Engineering Department, Faculty of Science and Engineering, University of Nusa Cendana, Kupang, Indonesia

¹nanojb@gmail.com

Abstract. The emergence on nanotechnology has driven the advancement of a lot of materials, one of which is nano-silica. Therefore, the research on the application of nano-silica in concrete has been conducted by researchers. The results showed that the strength and durability of concrete can be significantly increased by the application of nano-silica. However, the conducted research was limited to 28 days (short term). Furthermore, nano silica as a new material needs to be tested over a long period of time (more than 28 days) to determine its impact on concrete. Research on the long-term implications of using nano silica was carried out on f_c 45 MPa concrete. The percentage of nano silica used is fixed, at 5% of the weight of the binder. Furthermore, mechanical properties were tested including; compressive strength, tensile strength and slump test of normal concrete at 28, 56 and 91 days of the concrete'age. The results showed that the use of nano silica can increase compressive strength and tensile strength. The results showed that when compared to normal concrete, the use of nano silica can increase compressive and tensile strength and also produce better mechanical properties.

1. Introduction

Using nano-silica in a mixture of paste, mortar, and concrete greatly improves the mechanical properties and durability of concrete [1, 2]. The effect of using nano silica has received the attention of many researchers in recent years because nano silica has shown better performance compared to other additives [3]. Nano silica could fill the spaces between particles of gel C-S-H, acting as a nano-filler, and the pozzolanic activity of nano silica was very high, which increased the amount of C-S-H and resulted in higher densification of matrix, improving the strength and durability of concrete [4]. Nano silica is a relatively new material to be applied to high-performance concrete and the price is much higher compared to other pozzolanic materials, but it is very effective [5]. The researchers have sought to overcome the main disadvantage of fly Ash concrete with the addition of nano to cement and concrete paste to increase pozzolanic reactivity and early strength [6]. Percentage of nano silica used in concrete mixes will affect the mechanical properties in concrete, a low percentage of nano silica particles does not enhance the performance of mortar under long-term [7]. Percentage of nano silica 5-10% proved to be effective in increasing mechanical properties and durability of concrete [8, 9]. Nano silica is a highly reactive pozzolanic and could consume calcium hydroxide to form secondary Calcium silicate hydrate and improve cement composites properties through different mechanisms [10, 11]. There is a limited knowledge about the mechanism by which NS affects the settings times, workability, mechanical properties etc of concrete. Nano silica as a new material needs to be continuously researched both in the



laboratory scale and in the field. This is needed to better understand the behavior of nano silica in concrete. But unfortunately, research on the use of nano silica into a mixture of pasta, mortar, and concrete, is carried out at 28 days (short-term). For this reason, research on the long-term effects of using nano silica on concrete mechanical properties is important. In this study the effect of nano silica on mechanical properties in the form of compressive strength, tensile strength and slump for concrete f_c 45 MPa.

2. Materials and Method

The material used in this research was the type 1 ordinary portland cement, coarse aggregate, and fine aggregate from PT. Adhimix Precast Indonesia. The super-plasticizer used is the type of Polycarboxylate Ether Superplasticizer (PCE) from PT. John Idetama Teknik and nano silica type HDKN 20 from PT. Brataco with properties as shown in Table 1.

Table 1. Properties of nano silica HDKN 20

Properties	Unit	Value
Surface BET	m ² /g	197
pH-Value	No unit	4,0
Silicon dioxide	%	100
Sieve residue > 40 μ m	%	0,001
Loss on ignition	%	0,6
Content heavy metals	ppm	<25

While Table 2 shows the proportion of concrete mixture f_c 45 MPa in 1 m³, the specimen with BR code is normal concrete i.e. without nano-silica, BNS1 is concrete with the addition of 5% nano silica and 0.6% PCE, while the BNS2 concrete is made up of 5% nano silica and 3.5% PCE. Slump plan is 16 \pm 2 cm. Concrete mixing in nano silica BSN1 is mixed with silica sand, while nano silica BSN2 is mixed with cement first.

Table 2. The proportion of f_c 45 MPa concrete mix in 1 m³

Material	BR	BNS 1	BNS 2
OPC (kg/m ³)	580	580	580
Nano silica (kg/m ³)	-	29	29
Coarse Aggregate (kg/m ³)	1014	1014	1014
Fine Aggregate (kg/m ³)	595	595	595
Water/ binder	0.31	0.31	0.31
PCE (litre/m ³)	3.5	3.5	20.3

Figure 1 shows the specimen and curing done. The number of specimens for the press and pull examination are 3 for each concrete age specimen.



Figure 1. Specimen and curing

The specimen examination was carried out as shown in Figure 2. The examination was conducted by testing the slump with ASTM C 143-90 standard.



Figure 2. Testing of a slump (a), compressive strength (b) and tensile strength (c).

The compressive strength test refers to ASTM C39 and tensile strength refers to ASTM C496 / C496 M. The compressive strength examination was in form of a cylinder with 10 cm diameter and 20 cm height. The experiments conducted to test the compressive and tensile strength at 28, 56 and 91 days.

3. Results and Discussion

3.1. Slump Test

Slump test results as shown in Figure 3. BR 14 cm slump value. From the results of the slump examination, nano silica addition resulted in a decrease in the BNS1 slump value of 4cm. This slump value is in accordance with previous research, that addition 1,5 % NS significantly decreased the slump from 17,5 cm to 24 cm as reference slumps of concrete with $w/b = 0.65$ and 0.55 to 3 cm and 4 cm. [12]. The decrease in slump value is caused by the formation of the sort of structure that has high water retention after the addition of nano silica [13]. Furthermore, with the addition of 3.5% of PCE led to a slump value increased of 18 cm.

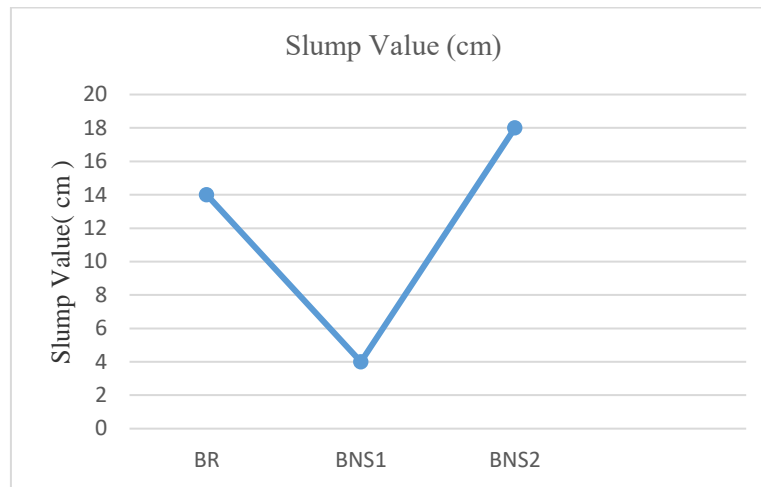


Figure 3. Slump value

From the conducted experiments, a conclusion can be drawn; to obtain a slump value of 16 ± 2 cm in nano-silica concrete requires 3.5% additional Polycarboxylate Ether Superplasticizer (PCE).

3.2. Compressive Strength

Figure 4 shows the results of compressive strength at 28, 56 and 91 days after mixing concrete at BR of 47 MPa, 49 MPa and 55 MPa. Whereas, BSN1 is 33 MPa, 36 MPa and 42 MPa. In BSN2, the compressive strength is 58 MPa, 65 MPa and 71 MPa. Based on the results of compressive strength with the addition of 5% of nano silica, fixed water/ binder 0.31 with 0.6% PCE, there was a decrease in compressive strength compared to concrete in reference. The decrease in compressive strength at 28, 56 and 91 days was 29.7%, 26.5%, and 23.4% respectively. This occurred because Agglomeration occurs [14]. However, agglomeration can be overcome by adding 3.5% of PCE with a percentage of by weight of cement. This can be seen from the value of the resulting slump and increased compressive strength compared to the concrete in reference. The percentage increase in compressive strength at BNS2 for 28 days of concrete age was 23.4%, 56 days at 32.7% and 91 days at 29%. There is a reduction in the amount of $\text{Ca}(\text{OH})_2$ for nano modified concrete indicating the formation of the additional C-S-H gel. From mechanical characterization of compressive strength. The SiO_2 in nanoscale behave not only as a filler to improve the microstructure but also as an activator to promote pozzolanic reactions. The influences and importance of superplasticizer while mixing cement with nanoparticles for mortar or concrete preparation were addressed [15, 16].

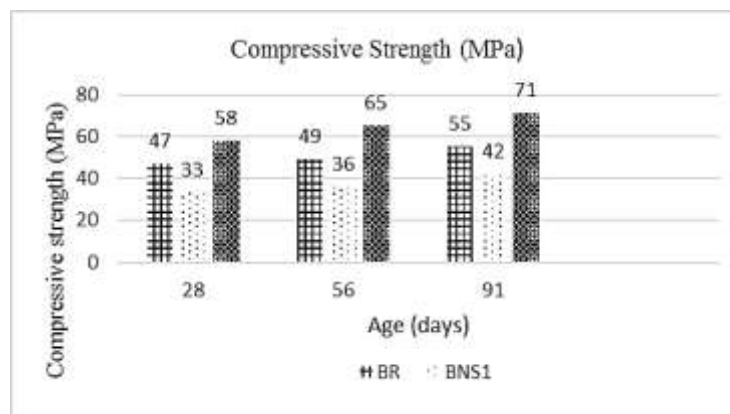


Figure 4. The Result of testing the Compressive strength

The results of compressive strength show that the long-term effect of nano silica has a similar performance to normal concrete, which increases with age of concrete.

3.3. Tensile Strength

The results of the concrete tensile strength at 28, 56 and 91 days is shown in Figure 5. The tensile strength of BR specimens at 28 days was 14.4 MPa and 56 days was 14.5 MPa. There was an increment of 0.7%. After 91 days, the tensile strength recorded was 16.9 MPa and this increased by 17.4%. The tensile strength for BNS1 at 28 days was 11.5 MPa and this decreased by 20.1%. At 56 days, the tensile strength was 12 MPa and this decreased by 17.2%. At 91 days, it was 14.9 MPa and this decreased by 11.8% from the concrete in reference. Meanwhile, in the BNS2 specimen, there was an increase in the tensile strength at 28 days by 47.9% to 21.3 MPa. At 56 days, it increased from 47.2% to 22.8% and at 91 days, a 40.8% increase from 16.9 MPa to 23.8 MPa. The results show that the addition of 5% of nano silica increased the concrete tensile strength in BSN2 and a decrease in BSN1 compared to BR.

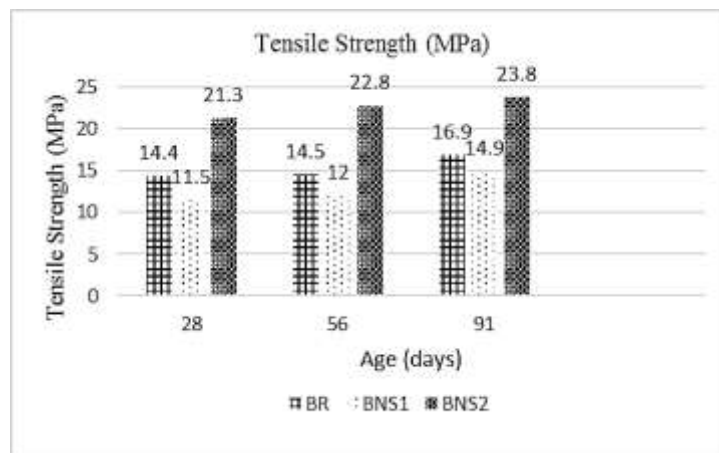


Figure 5. The Result of testing the Tensile strength

The increase in concrete compressive and tensile strength with the addition of 5% nano-silica, was influenced by the method of nano silica mixing. In BSN1, nano silica is stirred with fine aggregates, agglomeration occurs to inhibit chemical reactions. This results in a relative decrease in tensile strength. Whereas in BSN2, nano silica is mixed with cement first, enabling it to be dispersed well and this causes nano-silica to react perfectly. Therefore, this attribute can increase the compressive and tensile strength of the concrete.

4. Conclusion

1. The long-term effects of nano silica on concrete can improve its mechanical properties better than normal concrete.
2. The value of compressive strength can increase by 23.4% - 32.7% and tensile strength 40.8% - 47.2%.
3. The order to efficiently use nano silica, it must be mixed with cement first to produce a perfect reaction.

5. Acknowledgment

The author expressed his gratitude to KEMENRISTEKDIKTI for the assistance of research funding through a competency-based Grant scheme for the 2018 budget year.

6. References

- [1] Lok Pratap Singh, Anjali Goel, Srman Kumar Bhattacharyya, Saurabh Ahalawat, Usha Sharma, and Geetika Mishra. 2015 *International Journal of Concrete Structures and Material*

- 9 207-217
- [2] Hou P, Kawashiwa S, Wang K, Corr D, Qi J, and Shah S 2013 *Cement and Concrete Composites* **35** 12-22
 - [3] Sanchez F and Sobolev K 2010 *Construction and Building Materials* **24** 2060-2071
 - [4] Qing Y, Zhang Z, Kong D, Rongshen C 2007 *Construction and Building Materials* **21** 539-545
 - [5] Kong D, Su Y, Du X, Yang Y, Wei S, and Shah S 2013 *Construction and Building Materials* **43** 557-562
 - [6] Zhang M and Islam J 2012 *Construction and Building Materials* **29** 573-580
 - [7] Bolhassani M and Samani M 2014 *ACI Material Journal* **111** 1-6
 - [8] Eddhie J 2017 *International Journal of Technology* **4** 728-736
 - [9] Ehsani M, Nili M, Shaabani K 2017 *KSCE Journal of Civil Engineering* **21** 1854-1865
 - [10] J Song and S Liu 2016 *Advances in Material Science and Engineering* 1-7
 - [11] S Haruehansapong, T Pulngern, and S Chucheeepsakul 2015 *Construction and Building Materials* **50** 471-477.
 - [12] Isfahani F, Redaelli E, Lollini F 2016 *Advances in Materials Science and Engineering* 1-16
 - [13] R. Yu, P. Spiesz, and H. Brouwers 2014 *Construction and Building Materials* **65** 140-150
 - [14] Nili M. and Ehsani A 2015 *Materials & Design* **75** 174-183
 - [15] Byung W, Chang H, and Jae L 2007 *KSCE Journal of Civil Engineering* **11** 37-42
 - [16] Eddhie J 2017 *International Journal of Technology* **4** 728-736

Repair of rigid pavement using micro concrete material

Jonbi Jonbi^{1,*}, *A. R. Indra Tjahjani*¹, *Nuryani Tinumbia*¹, *A. M. Pattinaja*¹, and *Bambang S. Haryono*²

¹Civil Engineering Department, Faculty of Engineering, Pancasila University, Indonesia

²Civil Engineering Department, Faculty of Engineering, Tama Jagakarsa Indonesia

Abstract. Rapid setting materials, especially for concrete repairs made on major arteries such as toll roads which must withstand heavy traffic. Several manufacturers of construction chemicals have been producing various types of rapid setting materials designed for use in repairing such toll roads. However, the existing toll road repair materials have not demonstrated satisfactory performance when applied in the field. This study modified micro concrete materials by adding Polycarboxylate Ether (PCE) and Polypropylene Fiber (PPF) at the time of mixing existing rapid setting materials. It then tested flow tests and setting time at 16, 20, 30, 40, and 60 minutes, as well as compressive strength; and flexural strength tests at the ageing times of 3 hours, 1 day, and 7 days. The concrete micro material was applied directly in the field. The results show that micro concrete material is definitely suitable for toll road repair. The addition of PCE and PPF can increase the flexural strength and modulus of elasticity, meaning that the material is not easily cracked under the repeated strains of heavy traffic loads. Therefore, the use of this micro concrete material has been proven to be viable for future repairs of heavily trafficked toll roads.

1 Introduction

In Indonesia, new toll roads are being constructed rapidly and existing arteries are increasingly being expanded. However, once toll roads are built they often undergo structural damages, such as the Cipularang toll road which connects Jakarta to Bandung. The Cipularang toll road carries heavy traffic and a high volume of vehicles. Contours of the highway that climb sharply and turn abruptly, combined with unstable base soil factors and high amounts of rainfall, result in rapid erosion and other soil issues that cause damage to the road bed and pavement surfaces, including collapsing, pumping, and spalling, as illustrated in the following photos. One of the main obstacles to performing effective repairs is the requirement that these important highways should not be closed for very long during the repair process.

* Corresponding author: nanojbg@gmail.com



Fig. 1. Damage to the rigid pavement.

In addition, although high-early-strength cementitious repair materials are commercially available, many of these materials are especially vulnerable to cracking, poor bonding, and premature deterioration, which result from various causes such as incompatibility with the existing concrete pavement [1,2].

Satisfactory repair work requires materials with rapid setting criteria that have high compressive strength and flexure strength. These important characteristics ensure longer service life. Long service life means fewer future repairs as well as longer intervals between rehabilitation and reconstruction projects, leading to significant savings in both the quantity of pavement materials required and overall expenditures [3]. Some studies have shown there have been issues arising when using high-early-strength concrete in repair applications for pavements [4,5]. Therefore, it is essential that good-quality local materials that have the structural capabilities to conform to, or even exceed, the standard criteria for such repairs, should be developed as quickly as possible [6,7,8,9].

Polypropylene Fiber (PPF), shown in Figure 1, is a synthetic fiber with low density, fine diameter and low modulus of elasticity. It exhibits special characteristics such as high strength, high ductility, and durability. Polypropylene Fiber also demonstrates excellent bonding capabilities which can greatly improve the properties of mortar [10].



Fig. 2. Polypropylene Fiber.

This research developed micro concrete material in accordance with the criteria needed for effective repair work in the rigid pavement. This development was accomplished by adding superplasticizer and Polypropylene Fiber (PPF) to existing commercially available repair materials.

2 Materials and methods

Two types of materials were utilized in this research: Estopatch RSP and Patchroc RSP. Estopatch RSP is supplied by Estop Indonesia Corporation, and Patchroc RSP is supplied

by Fosroc Indonesia Corporation [11]. Both types of materials are fast-setting micro concrete, and are readily available commercial products. The fiber used, Polypropylene Fiber (PPF) supplied by Sika Indonesia Corporation, has the following properties: fiber length 12 mm; diameter 18 microns; tensile strength 300-400 MPa; elastic modulus 6000-9000 N/mm²; specific gravity 0.91 g/cm³. The superplasticizer used is Polycarboxylate Ether (PCE), supplied by John Hi-Tech Contrindo Corporation.

The mix proportions of each specimen are shown in Table 1. Specimen A0 is Estopatch RSP material; A1 is A0 plus 50 grams PPF (0.2% x A0), and A2 is A0 plus 50 grams PPF (0.2% xA0) and 0.25 litres superplasticizer PCE (1% x A0). Specimen B0 is Patchroc RSP; B1 is B0 plus 50 grams PPF (0.2% x B0) and B2 is B0 plus 50 grams PPF (0.2% xB0) and 0.25 litres superplasticizer PCE (1% x B0).

Table 1. Mix proportions of specimen.

Mix Proportions	Specimen					
	A0	A1	A2	B0	B1	B2
Binder (kg)	25	25	25	25	25	25
Water/binder	0.15	0.15	0.15	0.15	0.15	0.15
PPF (gram)	-	50	50	-	50	50
PCE (litre)	-	-	0.25	-	-	0.25

A compressive strength test of 50 x 50 x 50 mm cubes in accordance with ASTM C39 for concrete ages of 3 hours, 1 day and 7 days was recorded. Flexural testing of 50 x 50 x 30 mm prisms or beams in accordance with ASTM C78 / C78M-18 [12] were measured at ages of 3 hours and 1 day, while the initial setting time was recorded based on ASTM C403 / C 403-99 [13].



Fig. 2. Test equipment for specimens.

3 Results and discussion

3.1 Setting time

The result of the time setting test is shown in Figure 3. Material B0 sets faster compared to material A0. These results indicate that both materials are rapid setting, because they can harden in less than 60 minutes. Setting time is an important factor for cost-effective rigid pavement repairs, because reducing total work time (and highway usage down time) is critical when major highways are involved. Setting time also indicates when, and how

easily, a particular type of material can be applied. Significantly, including PPF in the concrete mixture does not have obvious negative effects on the setting times for either material, A0 and B0.

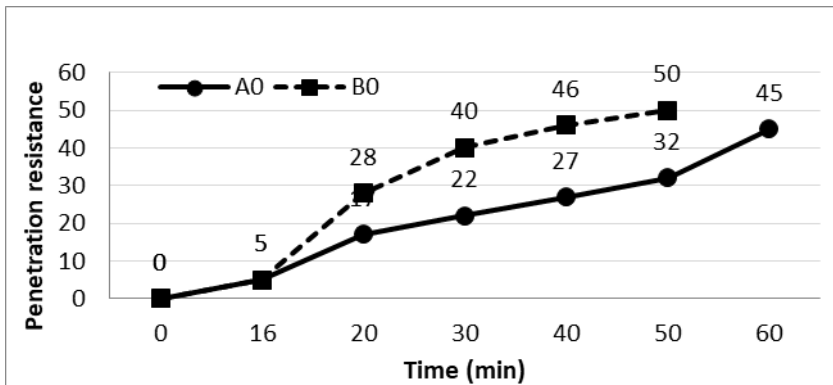


Fig. 3. Result of setting time test.

3.2 Compressive strength

The results of the compressive strength tests are shown in Figure 4. Significant improvements occurred with the addition of PPF as well as the addition of PPF and Admixture. At the age of 3 hours for A0: 22.2 MPa, A1: 23.1 MPa there is an increase of 4%, while for A2 of 24.3 MPa there is a 9.5% increase. For B1 specimens at 3 h, there was an increase of B0: 21.9 MPa to 22.9 MPa, 4.5% increase; B2 increased by 15% to 25.2 MPa. At the age of 1 day, on specimens A1 and A2 compressive strength increased by 2.9% and 24.3% respectively. As for B1 and B2, compression strength increased by 13.5% and 35.5%. 7-day age specimens exhibited an increase in compressive strength for A1 of 0.9%; A2 of 11.2%; B2 of 1.4%; and B2 of 9.9%. Based on the results of the compressive strength test, the addition of PPF and admixture can increase the compressive strength by 11.2% and 9.9%. This result is in line with previous research that states that adding polypropylene fibers to mortar can increase compressive strength and reduce plastic shrinkage cracks [14].

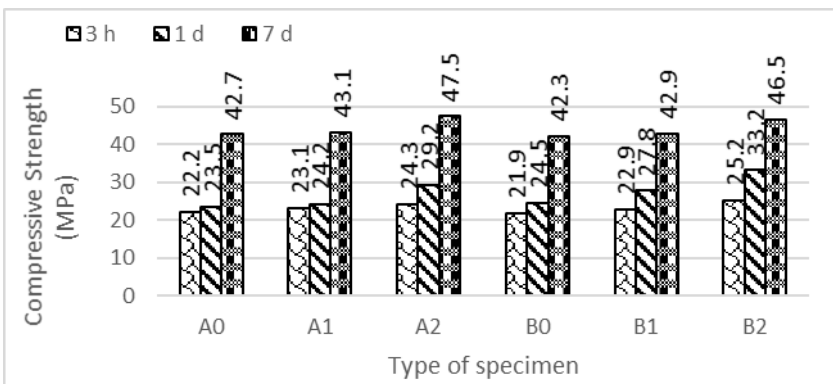


Fig. 4. Result of testing the compressive strength.

This enhancement may stem from improvements in the mechanical bond strength as the introduction of the ductile, durable fibers enable the concrete material to delay

micro-crack formation and even arrest their propagation afterwards to a certain extent [15]. Additionally, empirical evidence shows that the addition of superplasticizer can improve the workability of HPC due to the presence of PCE nanoparticles in the concrete slurry, which can fill any cavities within the concrete and thus result in strengthening of the bonds between the components of the mixture. [16].

Moreover, the use of fibers in the mortar or concrete can significantly enhance the bond strength between the old substrate and the new repair materials, which is one of the most important requirements for a successful repair [17].

3.2 Flexural strength

The flexural strength test results are shown in Figure 5. At an age of 3 hours, flexural strength in sample A0 is 3.1 MPa, which increased by 9.7% to 3.4 MPa in specimen A1. A2 increased by 22.6% to 3.8 MPa. Although for specimen B1 there is an increase of 12.5 MPa (B0: 3.2 MPa, B1: 3.6 MPa), for B2 there is an even larger increase of 25% to 4 MPa. At the age of 1 day, an increase of 58.3% was recorded. A0: 3.6 MPa; A1: 5.7 MPa; A2: 6.9 MPa (an increase of 91.7%). Specimen A0 at 7 days was 7.1 MPa; A1: 8.7 MPa (22.5%) and A2: 10.3 MPa (an increase of 18.4%). Then at 7 days, specimen B0 was recorded at 7.2 MPa; B1: 8.6 MPa (19.4%); B2: 10.4 MPa (44.4%).

The flexural test results show the addition of PPF and the effective admixture can improve the flexural strength in materials A0 and B0. This shows both A0 and B0 materials can be used as repair materials for rigid pavement roads, and the quality of the repairs would improve even more if combined with PPF and admixture.

As a further benefit, adding polypropylene fibers to the cement composites is also an effective method of preventing crack formation [18]. The short polypropylene fibers, when distributed uniformly throughout the entire volume of concrete, act to sew the edges of cracks together and restrict any further propagation [19]. Obviously, reduction of cracking is of great importance, especially in the first hours after pouring before the concrete reaches its full strength [20].

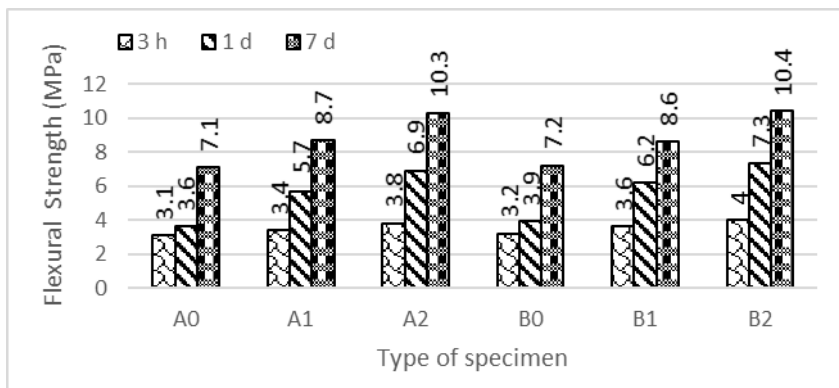


Fig. 5. Result of testing the flexural strength.

4 Conclusions

1. The use of either Polypropylene Fiber (PPF) or Polypropylene (PCE) is highly effective to improve the compressive strength and flexural strength of concrete mixtures used in repairing heavily trafficked road surfaces such as toll roads.

2. Adding PPF and PCE significantly improves the compressive strength by 11.2% and the flexural strength by 18.4% for material A0, and increases the compressive strength by 18.4% and flexural strength by 44.4% for material B0

The author thanks the financial support from Ministry of Research Technology and Higher Education of the Republic of Indonesia for this Research Grant with the Scheme of Penelitian Berbasis Kompetensi for the year 2018.

References

1. Li, M, Victor, C. L. *ACI Mater. J*, **108**, pp. 3-12 (2011)
2. H. Soliman, A. Shalaby, *Constr. Build. Mater*, **70**, pp. 148-157 (2014)
3. K. Hall, Federal Highway Administration, Washington, DC (2007)
4. C. Huang, S. Lin, C. Chang, H.C. Chen, *Constr. Build. Mater.* **46**, pp. 71-78. (2013)
5. D.P. Bentz, M.A. Peltz, *ACI Mater. J.* **105**. pp. 414-420 (2008)
6. J. Jonbi, B. Hariandja, I. Imran, I. Pane, *AMM*, **175-177**, pp. 1067-107 (2012)
7. J. Jonbi, B. Hariandja, I. Imran, I. Pane, **450-451**, pp. 277-280 (2012)
8. A.R.I. Tjahjani, J. Jonbi, R. Riadika, R. Mulyani, *AMR* **991-921**.pp 1836-1838. (2014)
9. H. Simatupang, *AIP Conf. Proc.* **1887**, 020028-1-020028-8 (2017)
10. S. Singh, A. Shukla, R. Brown, *Cem.Concr. Res.*, **34**, pp. 1919-1925, (2004)
11. Technical Book of Estopatch RSP ex PT. Estop; Patchroc RSP ex PT. Fosroc; PPF ex PT.Sika
12. American Society for Testing and Materials (ASTM). (2015)
13. American Society for Testing and Materials (ASTM). (1999)
14. Song, P-S., and C-J, Tu., *Journal of C.C.I.T.*, **43** (2014)
15. E. T. Dawood & M. Ramli, *Build Mater.* **24** 1043-1050 (2010)
16. Tan Rong Zhabf, Xiang Min Kong, Zhen Bao Lu, Zi Chen Lu, Shan Shan Hou, *Cem Concr Res* **67** (184-196) (2015)
17. C. Zanotti, N. Banthia, and G. Plizzari, *Cem.Concr.Res*, **63**, pp. 117-126 (2014)
18. Khaliq, W., and Kodur, V., *Cem. Concr. Res.***41**, pp. 1112-1122 (2014)
19. Alz T, Sanjazan JG, Collins F, *Mater, and Struct* **41**: 1741-1753 (2008)
20. Barluenga G, *Cem. Concr. Res* **40**: 802-809. 8 (2010)

Pengembangan Paving Geopolimer Berbahan Fly Ash

Jonbi

Prodi Teknik Sipil Fakultas Teknik Universitas Pancasila, E-mail: jonbi@univpancasila.ac.id

Partogi H.Simatupang

Prodi Teknik Sipil Fakultas Sains dan Teknik Universitas Nusa Cendana, Kupang, Provinsi NTT,
E-mail: partogihsimatupang@gmail.com

Detia Farah Ghina

Prodi Teknik Sipil Fakultas Teknik Universitas Pancasila, E-mail: detiafarahghina@gmail.com

Abstrak

Trend penelitian saat ini, lebih fokus pada bagaimana mengurangi penggunaan semen dan mengatasi masalah limbah industri salah satunya fly ash. Upaya yang dilakukann yakni mengembangkan geopolimer dengan fly ash sebagai bahan utama, dan menggunakan Natrium Hidroksida (NaOH) dan Sodium Silicate (Na_2SiO_3) sebagai activator. Tujuan dari penelitian ini adalah menghasilkan rasio NaOH : Na_2SiO_3 yang paling optimum dan menghasilkan paving block yang sesuai standar SNI. Dalam penelitian ini rasio activator NaOH : Na_2SiO_3 yang digunakan sebesar 1: 0,5 ; 1:1 ; 1:1,5 ; 1:2 dengan konsentrasi molaritas 11 M. Kemudian dibuat sampel uji berupa paving block dengan ukuran (200 x 110 x 80). Pengujian dilakukan kuat tekan pada umur ke 7, 14, dan 28 hari dan uji penyerapan air pada umur 28 hari. Hasil penelitian memperlihatkan rasio optimum activator adalah 1:2, menghasilkan paving block dengan kuat tekan dan workability yang tinggi. Kemudian rasio 1:1 ; 1:1,5 ; 1:2 memiliki kuat lebih dari 17 MPa termasuk mutu B dapat digunakan untuk area parkir. sedangkan rasio 1:0,5, menghasilkan paving mutu C dapat digunakan untuk pejalan kaki. Perbandingan harga paving geopolimer tersebut dengan harga paving berbahan semen yang beredar di pasaran juga turut dipresentasikan. Benefit dari penelitian ini, dapat menjadi salah satu solusi untuk mengatasi isu pencemaran lingkungan dan limbah industri..

Kata-kata Kunci: Paving Geopolimer, Fly Ash, Kuat Tekan, Penyerapan air.

Abstract

Current research trends are focused on reducing the use of cement and managing industrial waste, including fly ash, which is handled through its proper use as the main ingredient in geopolymers, along with Sodium Hydroxide (NaOH) and Sodium Silicate (Na_2SiO_3) as activators. This study, therefore, aims to produce the most optimal NaOH activator: Na_2SiO_3 ratio required in the production of concrete Paving block under the SNI standards, and those evaluated in this study include 1:0.5, 1:1, 1:1.5, and 1:2 with 11 molarity concentrations. In addition, the samples investigated were 200 x 110 x 80 cm concrete paving block, and compressive strength testing was performed on day 7, 14, and 28, while water absorption was assessed on a 28-day. The results showed 1:2 to be the optimal ratio, based on the high compressive strength and the superior workability of its concrete paving block. Furthermore, it was established that the activator ratios of 1:1, 1:1.5, 1:2 produced B-quality concrete paving block, with a compressive strength of 17 MPa, with possible application in a parking area. Also, the 1:0.5 preparations were of C quality with the probability of being used on the sidewalk. The comparison of the price of geopolymer paving and cement based paving is also presented. Thus, the study outcomes were candidates for adoption in the quest to overcome environmental pollution and industrial waste.

Keywords: Geopolymer Paving, Fly Ash, Compressive Strength, Water absorption.

1. Pendahuluan

Penggunaan semen sebagai pengikat pada campuran beton dan mortar berdampak negatif terhadap lingkungan. Data menunjukkan sebanyak 7% gas CO_2 yang ada di atmosfer berasal dari industri semen, karena memproduksi 1 ton semen akan menghasilkan 1 ton gas CO_2 ke dalam atmosfer dan menjadi salah satu pemicu pemanasan global [1,2]. Kemudian limbah dari PLTU berupa fly ash dan bottom ash yang berpotensi mencemari lingkungan dan termasuk limbah B3.

Berbagai penelitian inovasi telah dilakukan untuk mengurangi penggunaan semen atau tanpa menggunakan semen sama sekali dikenal sebagai geopolimer. Hasil penelitian menunjukkan bahwa geopolimer dapat menjadi salah satu solusi mengatasi limbah logam berat yang berbahaya dari industri modern dan dapat digunakan sebagai bahan pengganti semen [3,4].

Salah satu pemanfaatan perkembangan geopolimer dalam mengatasi masalah limbah Fly ash yakni dengan dijadikan sebagai paving block. Hal ini seiring dengan meningkatnya kebutuhan terhadap paving block karena memiliki beberapa keuntungan antara lain: ramah lingkungan dan sangat baik dalam membantu konsevasi air tanah, mudah dan cepat dalam pemasangan. Menurut peneliti lain Kemudian peneliti lain menyatakan bata

geopolimer dapat mengurangi emisi CO₂ hingga 59 % dibandingkan pembuatn batu bata dengan proses pembakaran [5].

Fly ash sangat potensial untuk dimanfaatkan sebagai bahan campuran paving block geopolimer karena mengandung nilai silica dan alumunia yang tinggi. Fly Ash yang digunakan diaktifkan dengan larutan alkali berupa Sodium Hidroksida (NaOH) dan Sodium Silikat (Na₂SiO₃) sebagai katalisatornya. Campuran aktivator NaOH dan Sodium silikat pada geopolimer lebih mudah dibuat dan ramah lingkungan dalam hal toksisitas dan leaching [6-13].

Larutan alkali tinggi digunakan untuk mengaktifkan fly ash untuk membentuk pasta yang mengikat aggerat kasar dan agregat halus dan bahan tidak bereaksi lainnya dicampurkan. Hasil penelitian mengungkapkan bahwa heatcured pada Geopolimer akan menghasilkan kuat tekan yang relatif tinggi, susut rendah, dan ketahanan yang baik terhadap sulfat dan asam [8].

Proses pembuatan paving block geopolimer dengan bahan fly ash diharapkan dapat mengurangi emisi CO₂ dan mengurangi limbah B3 fly ash. Saat ini kebutuhan paving block pada industri pekerasan area parkir mobil (mutu B) meningkat tinggi.

Tujuan dari penelitian ini adalah menentukan komposisi optimum variasi rasio Na₂SiO₃ yang menghasilkan kuat tekan dan workability tinggi. Penelitian paving block geopolimer meliputi pengujian sifat mekanik yakni kuat tekan BS 6717-1-1993, dengan persyaratan kuat tekan minimum 17 MPa untuk kategori paving block mutu B yang dapat di aplikasikan untuk area parkir mobil. Sedangkan mutu C, kuat tekan minimum 12.5 MPa untuk area pejalan kaki.[9]. Sedangkan persyaratan penyerapan air menurut SNI 03-0691-1996 untuk mutu B air rata-rata maksimum 6% , dan untuk mutu C sebesar 8% [10].

Benefit penelitian ini dapat menjadi salah satu alternatif mengatasi masalah semen dan fly ash menjadi material konstruksi berupa paving block geopolimer.

2. Material

Material yang digunakan pada penelitian ini adalah agregat kasar (kerikil) maksimum berukuran diameter 1 cm, agregat halus (pasir) dan fly ash tipe C berasal dari PT. Adhimix Precast Indonesia, Air berasal dari laboratorium PT. Adhimix Precast Indonesia, Alkali aktivator yang digunakan adalah Serpihan Natrium Hidroksida (NaOH) dan Larutan Sodium Silikat (Na₂SiO₃), pada Gambar 1.



Gambar 1. Material yang digunakan dalam penelitian

3. Metode Penelitian

Penelitian ini dilakukan dengan tahapan sebagai berikut: persiapan bahan baku, trial mix, membuat rancang campur paving block geopolimer, pembuatan benda uji, pengujian benda uji (uji kuat tekan dan penyerapan air), dan analisis hasil pengujian. Pembuatan benda uji paving block geopolimer dengan aktivator gabungan larutan NaOH dan Na₂SiO₃. Variasi rasio NaOH : Na₂SiO₃ sebesar 1:0,5 ; 1:1 ; 1:1,5 ; 1:2 dengan konsentrasi NaOH sebesar 11 M.

Berdasarkan pembuatan larutan yang telah dilakukan sebelumnya bahwa untuk pembuatan NaOH 11 M dapat secara praktis dilakukan dengan melarutkan 440 gram kepingan NaOH dengan 800 ml air suling (800 gram). Kemudian larutan NaOH 11 M dengan volume 1 liter tersebut didiamkan selama ± 24 jam, lalu direaksikan dengan Na₂SiO₃ sesuai dengan takaran per perbandingan seperti terlihat pada Gambar 2.

Pencampuran antara air dan serpihan NaOH harus dilakukan pada wadah tertutup dan di diamkan ± 6 jam, karena terjadi peningkatan suhu hingga 110° C. Fungsi dari di tutupnya wadah berisikan air dan serpihan NaOH atau yang di sebut alkali aktivator adalah menurunkan suhu campuran hingga 24°-27° C. Setelah itu larutan alkali activator di campurkan dengan Na₂SiO₃ yang berfungsi memperkuat ikatan polimerisasi. Pencampuran ini dapat meningkatkan suhu campuran hingga 40°, sehingga campuran harus di diamkan ± 6 jam dengan wadah tertutup. Hal ini berfungsi agar larutan activator yang nantinya akan dicampurkan dengan fly ash tidak terjadi gumpalan, dan dapat menyebabkan kegagalan dalam proses polimerisasi.



Gambar 2. Proses pembuatan larutan aktivator

Pada Tabel 1 terlihat proporsi campuran paving block geopolimer dengan variasi rasio activator.

Tabel 1. Proporsi campuran Paving Block Geopolimer

Fly Ash	Agregat		NaOH (M)	Variasi	Aktivator /FA
	Kasar	Halus			
1	1,36	2,53	11	1:0,5	0.37
1	1,36	2,53	11	1:1	0.32
1	1,36	2,53	11	1:1,5	0.28
1	1,36	2,53	11	1:2	0.25

Sedangkan untuk variasi rasio aktivator dan jumlah sampel paving block berukuran 200 x 110 x 80 mm dapat dilihat pada Tabel 2.

Tabel 2. Variasi rasio aktivator dan jumlah sample paving block

Variasi rasio Aktivator	Jumlah sampel (Buah)	Jumlah sampel berdasarkan Umur (Hari)		
		7	14	28
1:0,5	18	6	6	6
1:1	18	6	6	6
1:1,5	18	6	6	6
1:2	18	6	6	6

Pengujian yang dilakukan adalah pengujian kuat tekan pada umur 7, 14 dan 28 hari. Pengujian penyerapan air dengan cara perendaman juga dilakukan untuk paving yang berumur 28 hari. Pengujian yang dilakukan dalam penelitian ini diberikan pada Gambar 3 dan Gambar 4 berikut.



Gambar 3. Pengujian kuat tekan paving geopolimer



Gambar 4. Pengujian penyerapan air paving geopolimer

4. Hasil dan Pembahasan

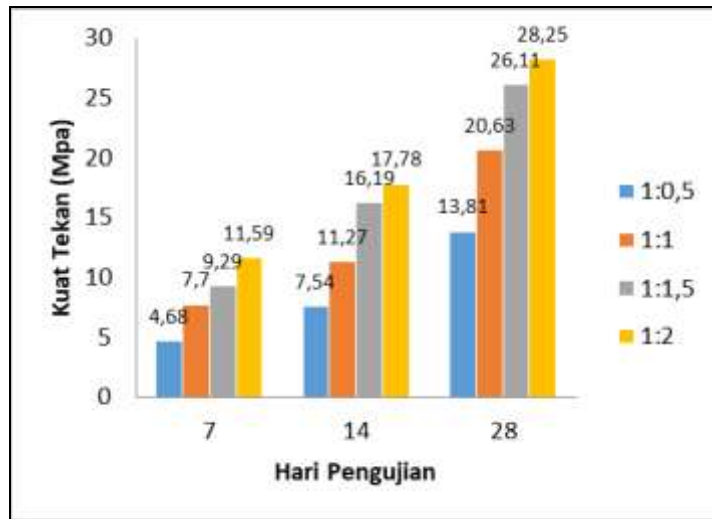
Paving geopolimer yang dihasilkan pada penelitian ini memiliki bentuk dan penampilan yang hampir sama dengan paving berbahan semen. Semakin banyak larutan natrium silikat (Na_2SiO_3) yang diberikan semakin baik dan halus permukaan paving yang dihasilkan. Berbagai produk paving geopolimer penelitian ini ditampilkan pada Gambar 5 berikut.



Gambar 5. Produk paving geopolimer yang dihasilkan

Pada Gambar 6. memperlihatkan hasil pengujian kuat tekan paving block geopolimer, nilai kuat tekan tertinggi pada umur 28 hari yaitu pada rasio 1:2 sebesar 28,25 MPa, dan nilai kuat tekan terendah pada rasio 1:0,5 yaitu 11,59 MPa. Peningkatan penambahan rasio 1:0,5 sampai 1:1 kuat tekan mengalami peningkatan masing-masing sebesar 6,82 MPa atau sebesar 33.06%, pada variasi 1:1 sampai 1:1,5 mengalami kenaikan sebesar 5,48 MPa atau sebesar 20.98% kemudian pada variasi 1:1,5 sampai 1:2 mengalami kenaikan kembali sebesar 2,14 MPa atau sebesar 7,57%. Hal ini menunjukkan penambahan rasio $\text{NaOH}:\text{Na}_2\text{SiO}_3$ dapat meningkatkan kuat tekan hal ini sejalan dengan penelitian sebelumnya [11,12].

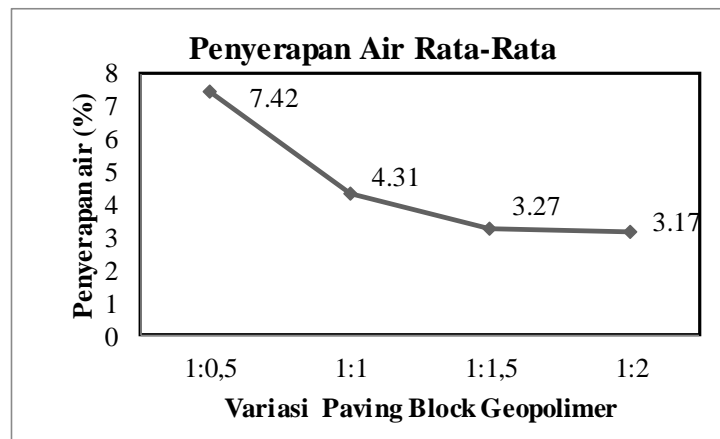
Hasil ini memperlihatkan paving block rasio activator sebesar 1:1 , 1:1,5 ,1:2 memenuhi persyaratan sebagai mutu B dapat diaplikasi pada area parkir. Sedangkan rasio activator untuk kategori mutu C untuk area pejalan kaki.



Gambar 6. Hubungan Umur Pengujian Terhadap Kuat Tekan Paving Block Geopolimer

Pada Gambar 7. memperlihatkan hasil uji penyerapan air, dengan rasio 1:0,5 menghasilkan penyerapan air tertinggi 7.42% dan rasio 1:2 terendah sebesar 3.17%. Peningkatan rasio Na_2SiO_3 akan menurunkan persentase penyerapan air. Dengan demikian rasio sebesar 1:0,5 1:2 rata-rata penyerapan air mengalami penurunan sebesar 41.90%, 24.12%, dan 3.06%.

Penyerapan air paving block dengan rasio 1:1, 1:1,5 dan 1:2 memiliki penyerapan air < 6 % mutu B yang dapat digunakan pada area parkir mobil. Sedangkan untuk rasio 1: 0.5 memiliki nilai penyerapan 7.42 % < 8% mutu C digunakan untuk area pejalan kaki.



Gambar 7. Hasil uji penyerapan air rata-rata paving block geopolimer

Perbandingan harga dilakukan dengan melakukan analisa harga paving geopolimer diberikan pada Tabel 3. Adapun campuran yang diambil adalah campuran 1:0.5 yang menghasilkan harga termurah.

Harga paving geopolimer dalam penelitian ini memiliki nilai paling murah sebesar Rp. 8.410,- per buah. Sementara harga paving block berbahan semen dipasaran yaitu berkisar Rp.2.500, per buah. Hal ini menunjukkan harga paving block geopolimer lebih mahal berkisar 3 s/d 4 kali harga paving block berbahan semen yang ada dipasaran. Komponen paling mahal dalam pembentuk harga paving geopolimer adalah harga larutan activator baik itu larutan natrium silikat maupun natrium hidroksida padat. Harga paving block geopolimer akan kompetitif dengan harga paving block yang ada dipasaran jika harga larutan activator tersebut dapat ditekan sekecil mungkin

Tabel 3. Analisa harga per unit paving block geopolimer

No.	Bahan	Volume	Satuan	Harga Satuan	Biaya
1	Fly Ash	0.56	kg	-	-
2	NaOH solid	0.11	kg	10.000	1.100
3	Air Suling	0.2	kg	1.000	200
4	Sodium Silikat (Na ₂ SiO ₃)	0.06	kg	10.000	600
5	Kerikil	0.76	kg	3.000	2.280
6	Agregat Halus	1.41	kg	3.000	4.230
TOTAL HARGA PER UNIT					8.410

5. Kesimpulan dan Saran

Komposisi optimum rasio aktivator NaOH : Na₂SiO₃ sebesar : 1: 2 yang menghasilkan kuat tekan dan workability tinggi. Paving Block yang dihasilkan pada rasio aktivator 1:1, 1:1,5 1:2 dapat digunakan untuk area parkir mobil (Mutu B). Paving Block dengan rasio aktivator sebesar 1: 0,5 dapat digunakan untuk pejalan kaki (mutu C).

Biaya paving block geopolimer belum kompetitif dibandingkan dengan harga paving berbahan semen yang ada dipasaran sekarang ini karena harga paving geopolimer masih sangat mahal yaitu berkisar 3 s/d 4 kali dibandingkan harga paving berbahan semen. Biaya larutan activator harus dapat ditekan sekecil mungkin agar dapat menghasilkan harga paving geopolimer yang kompetitif.

6. Daftar Pustaka

- A. Muthadi and V. Dhivya. Investigating Strength Properties of geopolimer Concrete with Quarry Dust. *ACI material journal*, V. 114. No.3. 2017. pp 355-363
- Al-Majidi, M. H., Lampropoulos, A., Cundy, A., and Meikle, S. Development of geopolimer mortar under ambient temperature for in situ applications. *Construction and Building Materials*, 2016, 120, pp.198-211
- BS 6717-1:1993, Precast concrete paving blocks. Specification for paving blocks
- Guo X, Hu W, Shi H. Microstructure and self solidification/stabilization (S/S) of Heavy metal of nano modified CFA-MSWIPA composite geopolimers *Constr. Build. Mater*, 2014 **56**, 81-86
- Hardjito, D.; Wallah, S. E.; Sumajouw, D. M. J.; and Rangan, B. V., "On the Development of Fly Ash-Based Geopolymer Concrete," *ACI Materials Journal*, V. 101, No. 6, Nov.-Dec. 2004, pp. 467-472
- Kumar, A. and Kumar, S. Development of paving blocks from synergistic use of red mud and fly ash using geopolimerization. *Construction and Building Materials*, 2013 38, pp.865-871
- Mali Basil, Study on Geopolymer concrete used for paving block, Department of Civil Engineering M G University, India, 2016
- Nguyen Van Chanh., Bui Dang Trung. Recent Reasearch in Geopolymer Concrete, 3nd ACF Internasional Conference. 2008, pp. 235-241
- Nicolas Youssef, Andry Zaid Rabenantoandro, Zakaria Dakhli, Fadi Hage Chehade, and Zoubeir Lafhaj. "Enviromental Evaluation of Geopolymer Bricks". *MATEC Web of Conferences* , France. INCER. 2019
- Simatupang, P.H., Imran, I., Pane, I., and Sunendar, B., On the Development of a Nomogram for Alkali Activated Fly Ash Material (AFAM) Mixtures . *J.Eng.Technol.Sci*, 2015, Vol 47.No.3, pp.231-249

Standar Nasional Indonesia untuk Paving Block. SNI-03-06910-1996. 1996. Bata Beton (paving block)

Temuujin, J; Van Riessen, A.; and William, R., "Influence of Calcium Compounds on the Mechanical Properties of Fly-Ash Geopolymer Concrete". *Journal of Materials in Civil Engineering, ASCE*, V. 27, No. 7, 2015, pp. 1-7. doi: 10.1061/(ASCE)MT.1943-5533.0001157

V. Bhiksha, M. Koti Reddy and t. Srinivas Rao. An Experimental Investigation On Properties Of Geopolymer Concrete (No Cement Concrete). *Asian Journal Of Civil Engineering, India* 2011. pp 842-853



Review

Application of the kinetic and isotherm models for better understanding of the behaviors of silver nanoparticles adsorption onto different adsorbents

Achmad Syafiuddin ^a, Salmiati Salmiati ^{a, b}, Jonbi Jonbi ^c, Mohamad Ali Fulazzaky ^{c, d, e, *}

^a Department of Environmental Engineering, Faculty of Civil Engineering, Universiti Teknologi Malaysia, 81310 UTM Skudai, Johor Bahru, Malaysia

^b Centre for Environmental Sustainability and Water Security, Research Institute for Sustainable Environment, Universiti Teknologi Malaysia, 81310 UTM Skudai, Johor Bahru, Malaysia

^c Faculty of Civil Engineering, Pancasila University, Jalan Kenseng Sawah, Jakarta 12640, Indonesia

^d Islamic Science Research Network, University of Muhammadiyah Prof Dr Hamka, Jalan Limau No. 2, Jakarta, 12130, Indonesia

^e Directorate General of Water Resources, Ministry of Public Works and Housing, Jalan Pattimura No. 20, Jakarta, 12110, Indonesia

ARTICLE INFO

Article history:

Received 20 November 2017

Received in revised form

12 March 2018

Accepted 14 March 2018

Keywords:

Adsorption isotherm model

Adsorption kinetic model

Arithmetic mean

Natural adsorbent

Silver nanoparticles

Synthetic adsorbent

ABSTRACT

It is the first time to do investigation the reliability and validity of thirty kinetic and isotherm models for describing the behaviors of adsorption of silver nanoparticles (AgNPs) onto different adsorbents. The purpose of this study is therefore to assess the most reliable models for the adsorption of AgNPs onto feasibility of an adsorbent. The fifteen kinetic models and fifteen isotherm models were used to test secondary data of AgNPs adsorption collected from the various data sources. The rankings of arithmetic mean were estimated based on the six statistical analysis methods of using a dedicated software of the MATLAB Optimization Toolbox with a least square curve fitting function. The use of fractal-like mixed 1, 2-order model for describing the adsorption kinetics and that of Fritz-Schlunder and Baudu models for describing the adsorption isotherms can be recommended as the most reliable models for AgNPs adsorption onto the natural and synthetic adsorbent materials. The application of thirty models have been identified for the adsorption of AgNPs to clarify the usefulness of both groups of the kinetic and isotherm equations in the rank order of the levels of accuracy, and this significantly contributes to understandability and usability of the proper models and makes to knowledge beyond the existing literatures.

© 2018 Elsevier Ltd. All rights reserved.

Contents

1. Introduction	60
2. Materials and methods	61
2.1. Data collection	61
2.2. Numerical simulation	61
2.2.1. Adsorption kinetic models	61
2.2.2. Adsorption isotherm models	62
2.3. Error analysis for application of the kinetic and isotherm models	63
3. Results and discussion	64
3.1. Results	64
3.1.1. Adsorption of AgNPs on glass beads	64
3.1.2. Adsorption of AgNPs on aged iron oxide magnetic particles	64
3.1.3. Adsorption of AgNPs on Fe ₃ O ₄ @ polydopamine core-shell microspheres	65

* Corresponding author. Directorate General of Water Resources, Ministry of Public Works and Housing, Jalan Pattimura No. 20, Jakarta, 12110, Indonesia.

E-mail address: fulazzaky@gmail.com (M.A. Fulazzaky).

3.1.4.	Adsorption of AgNPs on Poly(ethylenimine) functionalized core-shell magnetic	65
3.1.5.	Adsorption of AgNPs on <i>Aeromonas punctata</i>	65
3.2.	Discussion	66
3.2.1.	Application of the adsorption kinetic models	66
3.2.2.	Application of the adsorption isotherm models	66
4.	Conclusions	68
	Conflict of interest	69
	Acknowledgements	69
	Supplementary data	69
	References	69

1. Introduction

Silver nanoparticles (AgNPs) have been widely used in many industrial applications due to they have many advantageous properties of such as antibacterial, antifungal, antiviral, anti-inflammatory, anti-angiogenic and anticancer agents, as well as high electrical conductivity and high sensitivity (Desireddy et al., 2013; Kumar et al., 2008; Le Ouay and Stellacci, 2015; Naik et al., 2002; Park et al., 2012; Zhang et al., 2016). However, the excessive amount of AgNPs released from industrial products of such as detergents, textiles, toys, cosmetics and medical devices can have the potential to cause the risks to human health and the environment because of its antimicrobial effects and subsequent product applications, and the presence of AgNPs in the environment poses undesirable effects on plants of being inhibited seed germination and growth and has substantial adverse to microbial communities in engineered or natural ecosystems (Chen et al., 2017; Quadros and Marr, 2010; Tripathi et al., 2017). The content of AgNPs released from industrial products becomes more important and concerned in many countries because it can cause toxicity to aquatic biota near sources such as sewage discharges.

Adsorption found to be effective and cheap method among the available heavy metals removal methods and has been widely used to remove AgNPs from water. The use of nitrogen rich core-shell magnetic mesoporous silica as adsorbent has been proven to be effective for the removal of AgNPs from water with an adsorption capacity of 909.1 mg g⁻¹ (Zhang et al., 2017). The use of glass beads as adsorbent can remove up to 75% of AgNPs (Polowczyk et al., 2015). The use of aged iron oxide magnetic particles synthesized by a simple solvothermal method can remove up to 90% of AgNPs for a contact time of 90 min (Zhou et al., 2017). The elimination of AgNPs from synthetic wastewater by electrocoagulation has been proven to be effective by using four different routes (Matias et al., 2015).

Many theoretical and empirical models have been proposed for describing mechanisms of AgNPs adsorption from aqueous solution. However, the report provides practical guidance for choosing an appropriate method by comparing two, three or four models only. Four kinetic models of Lagergren pseudo-first-order, pseudo-second-order, Elovich and intraparticle diffusion have been tested for modeling the adsorption kinetics of AgNPs from aqueous solution to justify that two-parameter equations of pseudo-second-order showed more applicability than six-parameter equations of pseudo-first-order, Elovich and intraparticle diffusion (Ruíz-Baltazar et al., 2015). Application of four kinetics models and three isotherm models has been proposed for simulating the experimental data of AgNPs adsorption onto different adsorbents to show that all the data can have a better fit for both the kinetic model of pseudo-second-order and the isotherm model of Langmuir (Zhou et al., 2017). Two kinetic models (i.e., pseudo-first-order and pseudo-second-order) and three isotherm models (i.e.,

Dubinin-Radushkevich, Freundlich and Langmuir) have been proposed to test the experimental data of AgNPs adsorption and confirmed that using the pseudo-second-order and Langmuir models can get more accurate estimates of the parameter equations (Wu et al., 2017). The use of two kinetic models (i.e., pseudo-first-order and pseudo-second-order) and two isotherm models (i.e., Freundlich and Langmuir) has been used to simulate the experimental data of AgNPs adsorption to show that the most reliable estimates of the parameter equations were found with the pseudo-second-order and Langmuir models (Zhang et al., 2017). The use of Langmuir model has been proven to be better than that of Freundlich model for describing the adsorption of AgNPs on the surface of sodium montmorillonite nanoclays (Zarei and Barghak, 2015). Three models of pseudo-first-order, pseudo-second-order and Langmuir have been used to explain many observations in adsorption of AgNPs on the surface of a natural material of added *Aeromonas punctata* strain to show that the experimental data were fit well with the Langmuir and pseudo-second-order models (Khan et al., 2012). Modeling of experimental data for the adsorption of AgNPs from aqueous solution using the copper-based metal organic framework nanoparticles would fit well with the pseudo-second-order and Langmuir models, and the Langmuir isotherm does describe equilibrium behavior better than the Freundlich isotherm due to the adsorption does not continue beyond a monolayer (Conde-González et al., 2016). However, the experimental data for the adsorption of AgNPs on commercial activated carbon showed that the Freundlich isotherm can describe equilibrium behavior better than the Langmuir isotherm because of the adsorption continues beyond a monolayer (Gicheva and Yordanov, 2013). The conclusions obtained from different studies did show that the usefulness of statistical tests in model validation for the adsorption of AgNPs on the surface of a material is very limited.

The interpretation of adsorption isotherms has been reviewed for the applications of one one-parameter isotherm of Henry's model, thirteen two-parameter isotherms of Hill-Deboer, Fowler-Guggenheim, Langmuir, Freundlich, Dubinin-Radushkevich, Temkin, Flory-Huggins, Hill, Hasley, Harkin-Jura, Jovanovic, Elovich and Kiselev models, eight three-parameter isotherms of Redlich-Peterson, Sips, Toth, Koble-Carrigan, Kahn, Radke-Prausnits, Langmuir-Freundlich and Jossens models, four four-parameter isotherms of Fritz-Schlunder, Baudu, Weber-Van Vliet and Marczewski-Jaroniec models, and one five-parameter isotherm model developed by Fritz and Schlunder whereas the error analysis was performed using the nine methods of Sum of Square of Errors (ERRSQ), Hybrid Fractional Error Function (HYBRID), Average Relative Error (ARE), Marquardt's Percent Standard Deviation (MPSD), Sum of Absolute Errors (EABS), Sum of Normalized Errors (SNE), Coefficient of Determination (R^2), Nonlinear Chi-Square Test (X^2), Coefficient of Nondetermination ($1.00 - R^2$). This review concludes that the level of accuracy would be dependent on the successful modeling and interpretation of adsorption isotherms

(Ayawei et al., 2017). Even if the mass transfer factor (MTF) models to describe the adsorption kinetics of AgNPs solely in water (Fulazzaky, 2011, 2012) and the modified MTF models to describe the adsorption kinetics of AgNPs accompanied with multifarious solute in water (Fulazzaky et al., 2013, 2014; 2017) have not been used to possibly distinguish between the film mass transfer and the porous diffusion and to determine the resistance of mass transfer, it could be a challenge of verifying the possibility of using many other mathematical models to understand the behaviors of AgNPs adsorption. The aim of this study was to evaluate the use of fifteen kinetic models and that of fifteen isotherm models for describing the behaviors of AgNPs adsorption onto different adsorbents from aqueous solution. In the present work, the use of dedicated software program of the MATLAB Optimization Toolbox with a least square curve fitting (lsqcurvefit) function can be used as a framework to systematically manipulate and compare the application of six statistical methods of analysis toward a better understanding on the adsorption behaviors of AgNPs.

2. Materials and methods

2.1. Data collection

The data of AgNPs adsorption provided by secondary data sources were used as input to a numerical simulation process. The biological and non-biological adsorbent materials were all considered being testable in this study. The experimental data of AgNPs adsorption onto the synthetic materials of glass beads (GB) collected by Polowczyk et al. (2015), aged iron oxide magnetic particles (AIOMP) collected by Zhou et al. (2017), Fe₃O₄@ polydopamine core-shell microspheres (FPC) collected by Wu et al. (2017) and poly (ethylenimine) functionalized core-shell magnetic mesoporous silica composites (PFC) collected by Zhang et al. (2017) as well as those onto the natural (biological) material of using the strains of *Aeromonas punctata* (AP) collected by Khan et al. (2012) were reviewed to assess the reliability of a model and to compare different models.

2.2. Numerical simulation

2.2.1. Adsorption kinetic models

This study used the fifteen kinetic models to assess the behaviors of AgNPs adsorption onto different materials. To date, some of these models have been used as systemic approaches to simulate the secondary data (Khan et al., 2012; Polowczyk et al., 2015; Wu et al., 2017; Zhang et al., 2017; Zhou et al., 2017) in spite of many other models such as the MTF and modified MTF models (Fulazzaky, 2011, 2012; Fulazzaky et al., 2013, 2014; 2017) are still not considered for the analysis of the data.

In this work, the first-order model as proposed by Gupta et al. (2001) for dynamic modeling of lead and chromium removal from aqueous solution on red mud was used to assess the reasonableness of accounting its two-parameter equations and this can be mathematically written as follows:

$$q_t = q_e - \exp(-k_1 t) \quad (1)$$

where q_t is the adsorption capacity (mg g^{-1}) at time t (min), q_e is the adsorption capacity at equilibrium (mg g^{-1}), and k_1 is the first-order rate constant (min^{-1}).

The Ritchie second-order model has been used to describe the adsorption of cadmium ions from effluents using bone char (Cheung et al., 2001) and can be mathematically formulated (Cheung et al., 2001; Khambhaty et al., 2009) as:

$$q_t = \frac{q_e}{1 + q_e k_2 t} \quad (2)$$

where k_2 is the second-order rate constant (min^{-1}).

The pseudo-first-order model, firstly proposed by Lagergren (1898) to describe the kinetic process of liquid-solid phase adsorption of oxalic acid and malonic acid onto charcoal and then used by Ho and McKay (1998a) to describe the pseudo-first order sorption kinetics of phosphate onto tamarind nut shell activated carbon, can be mathematically written as the following formula:

$$q_t = q_e [1 - \exp(-k_{p1} t)] \quad (3)$$

where q_e is the adsorption capacity at equilibrium (mg g^{-1}), and k_{p1} is the pseudo-first-order rate constant (min^{-1}).

A kinetic model of the pseudo-second-order as proposed by Ho and McKay (1998b) to describe the chemisorption of divalent metal ions onto peat may be used to compare protocols and tests and this can be expressed as follows:

$$q_t = \frac{k_{p2} q_e^2 t}{1 + k_{p2} q_e t} \quad (4)$$

where k_{p2} is the pseudo-second-order rate constant (min^{-1}).

The intraparticle diffusion model (Plazinski and Rudzinski, 2009) to describe the transportation of species from the bulk to solid phase of porous material in solution may take the following form:

$$q_t = k_{ip} \sqrt{t} + c_{ip} \quad (5)$$

where k_{ip} is the measure of diffusion coefficient ($\text{mg g}^{-1} \text{min}^{-1/2}$) and c_{ip} is the intraparticle diffusion constant (mg g^{-1}).

A power model of describing the adsorption behaviors as proposed by Khambhaty et al. (2009) can be mathematically written as follows:

$$q_t = k_p t^{v_p} \quad (6)$$

where k_p and v_p are the power constants of the model.

The Avrami's model to describe the kinetics of phase transformation under the assumption of spatially random nucleation has been used for assessing the adsorption of either methylene blue or Hg(II) from aqueous solution (Lopes et al., 2003; Royer et al., 2009) and can be expressed by the following equation:

$$q_t = q_e [1 - \exp(-k_{av} t)^{n_{av}}] \quad (7)$$

where k_{av} the Avrami rate constant (min^{-1}) and n_{av} is the Avrami component (dimensionless).

The Bangham model has been used to describe the adsorption of anionic and cationic dyes on activated carbon from aqueous solution (Rodríguez et al., 2009) and can be written in the form of:

$$q_t = k_b t^{1/m} \quad (8)$$

where k_b is the adsorption rate constant ($\text{mg g}^{-1} \text{min}^{-1}$) and m is the indicator of adsorption intensity (dimensionless).

A kinetic model derived from the pseudo-first-order and pseudo-second-order called the mixed 1, 2-order model as proposed by Marczewski (2010) to assess the kinetics of dye adsorption onto mesoporous carbons from aqueous solution can be proposed in this work to assess the behaviors of AgNPs adsorption. The formula of the mixed 1, 2-order model can be written as follows:

$$q_t = q_e \frac{1 - \exp(-kt)}{1 - f_2 \exp(-kt)} \quad (9)$$

where f_2 is the mixed 1,2-order coefficient (dimensionless) and k is the adsorption rate constant ($\text{mg g}^{-1} \text{min}^{-1}$).

An exponential form of the kinetic equation (Haerifar and Azizian, 2013) can be used to describe the pattern of adsorption rate with time where its mathematical equation can be written in the following form:

$$q_t = q_e \ln[2.72 - 1.72 \exp(-k_e t)] \quad (10)$$

where k_e is the constant of the exponential model ($\text{mg g}^{-1} \text{min}^{-1}$).

A modified exponential model called as the fractal-like exponential model has been proposed by Haerifar and Azizian (2013) for the adsorption on heterogeneous solid surface and can be written in the form of:

$$q_t = q_e \ln[2.72 - 1.72 \exp(-k_{fle} t^\alpha)] \quad (11)$$

where k_{fle} is the fractal-like exponential rate coefficient ($\text{mg g}^{-1} \text{min}^{-1}$) and α is the constant of the model (dimensionless).

The Boyd's model as proposed by Kumar et al. (2014) to predict the actual slowest step in the adsorption process and by Viegas et al. (2014) for estimating intraparticle diffusion coefficients in adsorption processes can be used to assess the behaviors of AgNPs adsorption and this can be expressed as:

$$q_t = q_e \left[1 - \frac{6}{\pi^2} \exp(-Bt) \right] \quad (12)$$

where B is the coefficient that covers the effective diffusion process and radius of the particles (min^{-1}).

A modification of the pseudo-first-order model called as the Fractal-like pseudo-first-order model has been proposed by Haerifar and Azizian (2014) to introduce the fractal concept and can be written as:

$$q_t = q_e \left[1 - \exp(-k_{ffo} t^\alpha) \right] \quad (13)$$

where k_{ffo} is the fractal-like pseudo-first-order coefficient ($\text{mg g}^{-1} \text{min}^{-1}$) and α is the fractal-like pseudo-first-order model constant.

A modification of the pseudo-second-order model called as the fractal-like pseudo-second-order model proposed by Haerifar and Azizian (2014) to introduce the fractal concept can be mathematically written as:

$$q_t = \frac{k_{fso} q_e^2 t^\alpha}{1 + k_{fso} q_e t^\alpha} \quad (14)$$

where k_{fso} is the fractal-like pseudo-second-order coefficient ($\text{mg g}^{-1} \text{min}^{-1}$) and α is the fractal-like pseudo-second-order model constant.

A modification of the mixed 1, 2-order model called as the fractal-like mixed 1, 2-order model proposed by Haerifar and Azizian (2014) to introduce the fractal concept can be written in the mathematical expression of:

$$q_t = q_e \frac{1 - \exp(-k_{ffs} t^\alpha)}{1 - f_2 \exp(-k_{ffs} t^\alpha)} \quad (15)$$

where k_{ffs} is the fractal-like mixed 1, 2-order coefficient ($\text{mg g}^{-1} \text{min}^{-1}$) and α and f_2 are the fractal-like mixed 1, 2-order model

constants.

2.2.2. Adsorption isotherm models

To do a computation of performance of an adsorption system for selecting the most appropriate model, this study used the fifteen isotherm models to assess the behaviors of AgNPs adsorption onto different materials.

The Langmuir model proposed by Langmuir (1918) has been widely used to describe the adsorption occurred on homogenous surface by monolayer sorption with a finite number of identical sites such as for the adsorption of 2,4,6-trichlorophenol on coconut husk-based activated carbon (Hameed et al., 2008) and this can be mathematically expressed as:

$$q_e = \frac{K_L q_m C_e}{1 + K_L C_e} \quad (16)$$

where q_e is the adsorption capacity at equilibrium (mg g^{-1}), q_m is the maximum adsorption capacity per unit weight of the adsorbent (mg g^{-1}), C_e is the concentration of adsorbate at equilibrium (mg L^{-1}) and K_L is the Langmuir constant relating the affinity of the binding sites (L mg^{-1}).

The Freundlich model empirically developed by Freundlich (1906) would be suitable to describe sorption of several compounds to heterogeneous surfaces or surfaces supporting sites of varied affinities, assuming that stronger binding sites are occupied first and then binding strength decreases with increasing degree of site occupation (Silva et al., 2013), and can be expressed in the form of:

$$q_e = K_f C_e^{1/n} \quad (17)$$

where K_f is the Freundlich constant relating the sorption capacity (L g^{-1}) and n is the sorption intensity of adsorbent (dimensionless).

The Langmuir-Freundlich models would be suitable for describing both types of Langmuir and Freundlich adsorption isotherm (Jeppu and Clement, 2012) and can be written as:

$$q_e = \frac{q_m (K_a C_e)^n}{1 + (K_a C_e)^n} \quad (18)$$

where K_a is the affinity constant representing the degree of adsorption (L mg^{-1}) and n is the heterogeneity index.

The Redlich-Peterson model offers a compromise between two isotherm models of Langmuir and Freundlich by assuming the mechanism of adsorption is a hybrid and does not follow ideal monolayer adsorption (Wang et al., 2005) and can be formulated as follows:

$$q_e = \frac{K_{RP} C_e}{1 + a_{RP} C_e^b} \quad (19)$$

where K_{RP} and a_{RP} are the Redlich-Peterson isotherm constants (L g^{-1}) and b is the exponent that lies between 0 and 1.

The Toth model as empirical modification of the Langmuir model aims of reducing the error between experimental data and predicted values of equilibrium data (Ayawei et al., 2017; Sivarajasekar and Baskar, 2014) and can be written as:

$$q_e = \frac{q_m C_e}{(K_T + C_e^{n_T})^{n_T}} \quad (20)$$

where K_T is the Toth isotherm constant (mg g^{-1}) and n_T is the Toth model exponent (mg g^{-1}).

The Khan isotherm model has been used to describe the

experimental data with the minimum average percentage error for the adsorption of some pollutants from aqueous solutions by comparing several multicomponent adsorption isotherms (Ayawei et al., 2017; Khan et al., 1997) and can be expressed in the generalized mathematical expression of:

$$q_e = \frac{q_m b_K C_e}{(1 + b_K C_e)^{a_K}} \quad (21)$$

where b_K is the Khan isotherm constant ($L\ mg^{-1}$) and a_K is the Khan isotherm model exponent.

The Jovanovic model developed based on the assumptions contained in the Langmuir model with the possibility of some mechanical contacts between the adsorbing and desorbing molecules (Ayawei et al., 2017; Shahbeig et al., 2013) and can be formulated as follows:

$$q_e = q_m [1 - \exp(-K_J C_e)] \quad (22)$$

where K_J is the Jovanovic constant ($L\ g^{-1}$).

The Koble–Corrigan model proposed by Koble and Corrigan (1952) as a three-parameter equation of isotherm model which incorporates both Langmuir and Freundlich isotherms for representing equilibrium data of adsorption on heterogeneous surfaces (Ayawei et al., 2017; Shahbeig et al., 2013) and can be represented by the following formula:

$$q_e = \frac{q_m a C_e^d}{1 + b C_e^d} \quad (23)$$

where a , b , and d are the Koble–Corrigan isotherm constants.

The Rake–Prausnitz model developed based on the concept of thermodynamic ideal solution by Radke and Prausnitz (1972) has several important properties which makes it more preferred in most adsorption systems to low adsorbate concentration (Ayawei et al., 2017; Sivarajasekar and Baskar, 2014) and can be expressed as:

$$q_e = \frac{q_m a_{RP} C_e}{[1 + a_{RP} C_e]^{n_{RP}}} \quad (24)$$

where a_{RP} is the Radke–Prausnitz equilibrium constant ($L\ mg^{-1}$) and n_{RP} is the Radke–Prausnitz model exponent.

The Fritz–Schlunder model proposed by Fritz and Schlunder (1974) as an empirical equation can fit a wide range of experimental data (Ayawei et al., 2017) and can be expressed as follows:

$$q_e = \frac{a_{FS} C_e^{c_{FS}}}{1 + b_{FS} C_e^{d_{FS}}} \quad (25)$$

where a_{FS} and b_{FS} are the Fritz–Schlunder equilibrium constants ($L\ g^{-1}$) and c_{FS} and d_{FS} are the Fritz–Schlunder model exponents.

The Baudu model developed from the estimation of the Langmuir coefficients model by the measurements of tangents at different equilibrium concentrations (Ayawei et al., 2017; McKay et al., 2014; Sivarajasekar and Baskar, 2014) can be expressed as follows:

$$q_e = \frac{q_m b_B C_e^{1+x+y}}{1 + b_B C_e^{1+x}} \quad (26)$$

where b_B is the Baudu equilibrium constant ($L\ mg^{-1}$), x and y are the Baudu model parameters.

The Marczewski–Jaroniec model known as the four-parameter general Langmuir equation has been developed on basis the

distribution of the supposition of local Langmuir isotherm and adsorption energies distribution in the active sites on adsorbent (Chen, 2003; Sivarajasekar and Baskar, 2014) and can be expressed by the following formula:

$$q_e = \left[\frac{q_m a_{MJ} C_e^{b_{MJ}}}{1 + a_{MJ} C_e^{b_{MJ}}} \right]^{m_{MJ}/b_{MJ}} \quad (27)$$

where a_{MJ} is the Marczewski–Jaroniec equilibrium constant ($L\ mg^{-1}$) and b_{MJ} and m_{MJ} are the Marczewski–Jaroniec model exponents.

The Hill model developed by Hill (1910) based on the assumption that adsorption is a cooperative phenomenon with adsorbates at one site of the adsorbent influencing different binding sites on the same adsorbent (Rania and Yousef, 2015) can describe the binding of different solutes onto homogeneous adsorbent and can be written as:

$$q_e = \frac{q_m C_e^{n_H}}{K_H + C_e^{n_H}} \quad (28)$$

where K_H is the Hill isotherm constant and n_H is the Hill coefficient. Notes that the values of $n_H > 1$, $n_H = 1$ and $n_H < 1$ indicate positive cooperativity, non-cooperative or hyperbolic binding and negative cooperativity in binding, respectively.

The Brouers–Sotolongo model is an adsorption isotherm model given by a deformed exponential function of Weibull distribution (Podder and Majumder, 2016) and this can be written by the following formula:

$$q_e = q_m [1 - \exp(-K_{BS} C_e^{n_{BS}})] \quad (29)$$

where K_{BS} is the Brouers–Sotolongo equilibrium constant ($L\ mg^{-1}$) and n_{BS} is the Brouers–Sotolongo model exponent.

The Unilin model is one of the empirical correlations to express experimental data for representing the adsorption (Valenzuela and Myers, 1989) and can be mathematically formulated as follows:

$$q_e = \frac{q_m}{2b_U} \ln \left(\frac{a_U + C_e \exp(b_U)}{a_U + C_e \exp(-b_U)} \right) \quad (30)$$

where a_U is the Unilin equilibrium constant and b_U is the Unilin model exponent.

2.3. Error analysis for application of the kinetic and isotherm models

This study used the dedicated software of the MATLAB Optimization Toolbox with its lsqcurvefit function to simulate and analyze the experimental data of AgNPs adsorption on the natural and synthetic adsorbent materials. The algorithms can perform calculation, data processing and automated reasoning tasks based on the nonlinear lsqcurvefit function found in the MATLAB to find the coefficient of determination (R^2), root mean squared error (RMSE), percentage of error in maximum estimated value (E_{max}), percentage of error in minimum estimated value (E_{min}), mean absolute percent error (MAPE) and mean absolute deviation (MAD) for statistical analysis significance tests for all the kinetic and isotherm models. The first condition induces a ranking of the arithmetic mean for every model in terms of accuracy. Because of the arithmetic mean is the most commonly used and readily understood measure of central tendency, the selection of a potential model with comparison of the other models as a function of the number of terms in each model is based on the arithmetic mean

information criteria. Finally, the best model order can be determined using the minimum value of average ranking (AR). The mathematical equation of the statistical analysis methods can be described as follows:

(1) For the coefficient of determination,

$$R^2 = 1 - \frac{\sum (x_{obs,i} - x_{model,i})^2}{\sum (x_{obs,i} - \bar{x}_{obs})^2} \quad (31)$$

(2) For the root mean squared error,

$$RMSE = \sqrt{\frac{\sum_{i=1}^n (x_{obs,i} - x_{model,i})^2}{n}} \quad (32)$$

(3) For the percentage of error in maximum estimated value,

$$E_{max} = \left| \frac{x_{model,max} - x_{obs,max}}{x_{obs,max}} \right| \times 100\% \quad (33)$$

(4) For the percentage of error in minimum estimated value,

$$E_{min} = \left| \frac{x_{model,min} - x_{obs,min}}{x_{obs,min}} \right| \times 100\% \quad (34)$$

(5) For the mean absolute percent error,

$$MAPE = \left(\frac{1}{n} \sum \frac{|x_{obs,i} - x_{model,i}|}{|x_{obs,i}|} \right) \times 100\% \quad (35)$$

(6) For the mean absolute deviation,

$$MAD = \frac{1}{n} \sum |x_{obs,i} - x_{model,i}| \quad (36)$$

where $x_{obs,i}$ is the data obtained from observation at time i , $x_{model,i}$ is the data modeled for observation at time i , n is the number of data, $x_{model,max}$ is the maximum value of the modeled data, $x_{obs,max}$ is the maximum value of the observed data, $x_{model,min}$ is the minimum value of the modeled data, and $x_{obs,min}$ is the minimum value of the observed data.

3. Results and discussion

3.1. Results

The requirement to define a proper model for the adsorption of AgNPs onto different adsorbents has been becoming a concern in terms of AgNPs removal (Sheng and Liu, 2017). In this work, the following criteria were used to rank the goodness-of-fit testing of the kinetic and isotherm models to experimental data that the value of $AR < 3.75$, that of $3.75 \leq AR \leq 7.50$, that of $7.50 < AR \leq 11.25$ and that of $11.25 < AR \leq 15$ represent the very good, good, satisfactory and poor adsorption performance, respectively. The results of ranking the values of every statistical analysis method for the adsorption of AgNPs onto different adsorbents were analyzed on the basis of measuring the values of the parameter equations of each model (see Tables 1 and 2 in Supplementary materials) and can be then used to verify if one kinetic or isotherm model could fit the data better than others.

3.1.1. Adsorption of AgNPs on glass beads

The results (Table 3 in Supplementary materials) of ranking the values of arithmetic mean being obtained from every statistical analysis method for the kinetic models of AgNPs adsorption on GB show that the statistical analysis for the fractal-like mixed 1, 2-

order, fractal-like pseudo-first-order and fractal-like exponential models gives a very good fit to experimental data as their AR values of 1.2, 2.3 and 3.3, respectively, have been verified with a best fit being obtained for the fractal-like mixed 1, 2-order model due to its lowest AR value of 1.2. A good fit can be obtained for the fractal-like pseudo-second-order, Power, Boyd and Bangham models as their AR values of 3.8, 5.5, 5.7 and 6.2, respectively, were verified. The model-data fit can be considered satisfactory for the intraparticle diffusion, pseudo-second-order, mixed 1, 2-order and exponential models since the AR values were verified as high as 8.3, 9.3, 9.3 and 11.2, respectively. The statistical analysis for the pseudo-first-order, first order, Avrami and second-order models gives a poor fit to the data due to their AR values of 13.0, 13.2, 13.3 and 14.3, respectively, were verified and this reveals a very poor fit being obtained for the second-order model because of its AR value of 14.3 is higher than others.

The analysis of using the values of arithmetic mean for the isotherm models of AgNPs adsorption on GB (see Table 4 in Supplementary materials) shows that the Fritz-Schlunder and Baudu models give a very good fit to experimental data as their AR values of 1.67 and 2.67, respectively, have been verified with a best fit being obtained for the Fritz-Schlunder model verified by its lowest AR value of 1.67. A good fit can be found for the Khan, Toth and Radke-Prausnitz models as it can be verified by observation of their AR values of 3.67, 4.17 and 4.67, respectively. The verification of model-data fit carried out using the Brouers-Sotolongo, Hill, Redlich-Peterson, Jovanovic, Maczewski-Jaroniec, Koble-Corrigan and Langmuir models can be considered satisfactory since this view deals with the AR values as high as 7.67, 8.00, 8.17, 9.33, 10.00, 10.38 and 11.17, respectively. The statistical data analysis gives a poor fit for the Langmuir-Freudlich, Unilin and Freundlich models as it has been verified by the observation of the AR values as high as 12.00, 12.17 and 13.83, respectively, and this verification reveals a very poor fit for the Freundlich model due to its AR value of 13.83 is higher than others.

3.1.2. Adsorption of AgNPs on aged iron oxide magnetic particles

The results (Table 5 in Supplementary materials) of numerical simulation by the kinetic models of AgNPs adsorption on AIOMP show that the statistical analysis for the fractal-like mixed 1, 2-order, mixed 1, 2-order and fractal-like pseudo-first-order kinetic models gives a very good fit to experimental data as their AR values of 1.33, 1.83 and 2.83, respectively, have been verified with a best fit being obtained for the fractal-like mixed 1, 2-order model due to its lowest AR value of 1.33. A good fit can be obtained for the fractal-like exponential, fractal-like pseudo-second-order, pseudo-first-order and Avrami models since their AR values of 4.00, 5.00, 6.33 and 7.00, respectively, were verified. The model-data fit can be considered satisfactory for the exponential, pseudo-second order and power models because of the AR values were verified as high as 8.17, 9.17 and 10.67, respectively. The statistical analysis for the Bangham, Boyd, intraparticle diffusion, first-order and second-order models gives a poor fit to the data due to their AR values of 11.33, 11.33, 12.00, 14.33 and 14.67, respectively, were verified and this reveals a very poor fit being obtained for the second-order model because of its AR value of 14.67 is higher than others.

The analysis of using the values of arithmetic mean for the isotherm models of AgNPs adsorption on AIOMP (see Table 6 in Supplementary materials) shows that the only Brouers-Sotolongo model gives a very good fit to experimental data due to its AR value of 1.00 has been verified. A good fit can be found for the Langmuir-Freudlich, Fritz-Schlunder, Baudu, Koble-Corrigan, Hill, Maczewski-Jaroniec and Jovanovic models as it can be verified by observation of their AR values of 4.00, 4.50, 4.50, 4.67, 4.83, 5.50 and 7.00, respectively. The verification of model-data fit carried out

using the Toth, Khan and Radke-Prausnitz models can be considered satisfactory since this view deals with the AR values as high as 9.67, 9.83 and 10.50, respectively. The statistical data analysis gives a poor fit for the Langmuir, Unilin, Redlich-Peterson and Freundlich models as it has been verified by the observation of the AR values as high as 12.33, 12.67, 14.33 and 14.67, respectively, and this verification reveals a very poor fit for the Freundlich model due to its AR value of 14.67 is higher than others.

3.1.3. Adsorption of AgNPs on Fe_3O_4 @ polydopamine core-shell microspheres

The results (Table 7 in Supplementary materials) of ranking the values of arithmetic mean being obtained from every statistical analysis method for the kinetic models of AgNPs adsorption on FPC show that the statistical analysis for the fractal-like mixed 1, 2-order and pseudo-second order models gives a very good fit to experimental data because of their AR values of 1.17 and 2.83, respectively, have been verified with a best fit being obtained for the fractal-like mixed 1, 2-order model due to its lowest AR value of 1.17. A good fit can be obtained for the pseudo-first-order, first order, exponential, Boyd and Avrami models since their AR values of 4.83, 5.17, 5.33, 5.33 and 5.83, respectively, were verified. The model-data fit can be considered satisfactory for the fractal-like exponential, Bangham, power, fractal-like pseudo-first-order and mixed 1, 2-order models since their AR values were verified as high as 9.33, 10.00, 10.17, 10, 50, and 11.17, respectively. The statistical analysis for the fractal-like pseudo-second-order, intraparticle diffusion and second-order models gives a poor fit to the data because of their AR values of 11.50, 12.17 and 14.67, respectively, were verified and this reveals a very poor fit being obtained for the second-order model due to its AR value of 14.67 is higher than others.

The analysis of using the values of arithmetic mean for the isotherm models of AgNPs adsorption on FPC (see Table 8 in Supplementary materials) shows that the only Koble-Corrigan model give a very good fit to experimental data as its AR value of 2.17 has been verified. A good fit can be found for the Toth, Khan, Brouers-Sotolongo, Fritz-Schlunder, Baudu, Langmuir-Freundlich and Maczewski-Jaroniec models as it can be verified by observation of their AR values of 3.67, 4.00, 5.17, 6.33, 6.33, 6.67 and 7.00, respectively. The verification of model-data fit carried out using the Hill, Jovanovic and Langmuir models can be considered satisfactory since this view deals with their AR values as high as 9.33, 9.50 and 9.83, respectively. The statistical data analysis gives a poor fit for the Unilin, Radke-Prausnitz, Freundlich and Redlich-Peterson models as it has been verified by the observation of the AR values as high as 12.17, 12.33, 12.50 and 13.00, respectively, and this verification reveals a very poor fit for the Redlich-Peterson model due to its AR value of 13.00 is higher than others.

3.1.4. Adsorption of AgNPs on Poly(ethylenimine) functionalized core-shell magnetic

The results (Table 9 in Supplementary materials) of ranking the values of arithmetic mean being obtained from every statistical analysis method for the kinetic models of AgNPs adsorption on PFC show that the statistical analysis for the fractal-like pseudo-first-order, fractal-like mixed 1, 2-order and fractal-like exponential models gives a very good fit to experimental data as their AR values of 2.00, 2.83 and 3.17, respectively, have been verified with a best fit being obtained for the fractal-like pseudo-first-order model because of its lowest AR value of 2.00. A good fit can be obtained for the fractal-like pseudo-second-order, Boyd, pseudo-second-order, power and mixed 1, 2-order models as their AR values of 4.17, 5.83, 6.67, 7.00 and 7.00, respectively, were verified. The model-data fit can be considered satisfactory for the Bangham, intraparticle diffusion and exponential models since the AR values were

verified as high as 7.67, 10.33 and 10.33, respectively. The statistical analysis for the pseudo-first-order, Avrami, first-order and second-order models gives a poor fit to the data due to their AR values of 11.67, 12.33, 14.50 and 14.50, respectively, were verified and this reveals a very poor fit being obtained for the first-order and second-order model because of the same their AR value of 14.50 is higher than others.

The analysis of using the values of arithmetic mean for the isotherm models of AgNPs adsorption on PFC (see Table 10 in Supplementary materials) shows that the only Freundlich model give a very good fit to experimental data as its AR value of 3.67 has been verified. A good fit can be found for the Radke-Prausnitz, Toth, Fritz-Schlunder, Khan, Brouers-Sotolongo, Koble-Corrigan and Baudu models as it can be verified by observation of their AR values of 4.33, 4.50, 5.33, 5.50, 6.67, 7.17 and 7.33, respectively. The verification of model-data fit carried out using the Langmuir-Freundlich, Maczewski-Jaroniec and Unilin models can be considered satisfactory since this view deals with the AR values as high as 8.00, 8.67 and 9.33, respectively. The statistical data analysis gives a poor fit for the Jovanovic, Langmuir, Hill and Redlich-Peterson models since it has been verified by the observation of the AR values as high as 11.83, 12.50, 12.50 and 12.67, respectively, and this verification reveals a very poor fit for the Redlich-Peterson model due to its AR value of 12.67 is higher than others.

3.1.5. Adsorption of AgNPs on *Aeromonas punctata*

The results (Table 11 in Supplementary materials) of ranking the values of arithmetic mean being obtained from every statistical analysis method for the kinetic models of AgNPs adsorption on AP show that the statistical analysis for the fractal-like mixed 1, 2-order, fractal-like pseudo-first-order and fractal-like exponential models gives a very good fit to experimental data because of their AR values of 1.5, 2.3 and 3.5, respectively, have been verified with a best fit being obtained for the fractal-like mixed 1, 2-order model due to its lowest AR value of 1.5. A good fit can be obtained for the mixed 1, 2-order, fractal-like pseudo-second-order, pseudo-first-order and exponential models as their AR values of 5.7, 5.8, 5.7, 7.3 and 7.5, respectively, were verified. The model-data fit can be considered satisfactory for the Avrami, power, Bangham, pseudo-second-order and intraparticle diffusion models since the AR values were verified as high as 8.3, 8.7, 9.7, 10.3 and 10.7, respectively. The statistical analysis for the Boyd, second-order and first-order models gives a poor fit to the data due to their AR values of 11.5, 13.5 and 13.7, respectively, were verified and this reveals a very poor fit being obtained for the first-order model because of its AR value of 13.7 is higher than others.

The analysis of using the values of arithmetic mean for the isotherm models of AgNPs adsorption on GB (see Table 12 in Supplementary materials) shows that the Maczewski-Jaroniec, Brouers-Sotolongo, Fritz-Schlunder and Baudu models give a very good fit to experimental data since their AR values of 1.33, 2.17, 3.00 and 3.50, respectively, have been verified with a best fit being obtained for the Maczewski-Jaroniec model as verified by its lowest AR value of 1.33. A good fit can be found for the Unilin, Langmuir-Freundlich and Koble-Corrigan models as it can be verified by observation of their AR values of 5.33, 6.50 and 6.50, respectively. The verification of model-data fit carried out using the Hill, Toth, Khan, Langmuir, Jovanovic and Radke-Prausnitz models can be considered satisfactory since this view deals with their AR values as high as 7.50, 9.50, 10.00, 11.00, 11.00 and 11.00, respectively. The statistical data analysis gives a poor fit for the Freundlich and Redlich-Peterson models as it has been verified by observation of the AR values as high as 13.50 and 15.00, respectively, and this verification reveals a very poor fit for the Redlich-Peterson model due to its AR value of 15.00 is higher than others.

3.2. Discussion

3.2.1. Application of the adsorption kinetic models

The error analysis has been one of the most applied tools for defining the best fitting adsorption models because it consists of different statistical methods for determining the values of such as R^2 , RMSE, E_{max} , E_{min} , MAPE and MAD (Ayawei et al., 2017; Madhavan et al., 2016; Sivarajasekar and Baskar, 2014). This analysis induces a ranking of the arithmetic mean in term of accuracy for every model. The results (Tables 3, 5, 7, 9, 11 in Supplementary materials) show that the adsorption kinetic models for the adsorption of AgNPs do fit to the experimental data depending on type of the adsorbent. It is an inconsistency in the representational content of different models for the adsorption of AgNPs from aqueous solution and spectrum of the stimulating zone depends on AgNPs properties and environmental conditions (Sheng and Liu, 2017). The experimental evidence of the existence of fractal-like mixed 1, 2-order model for modeling the adsorption of AgNPs on GB, AIOMP, FPC, PFC and AP gives a very good fit to the data as judged by all the AR values of below than 3.75 in spite of the analysis of using the values of E_{max} , E_{min} and MAPE as high as 4.00 for the adsorption of AgNPs on PFC from aqueous solution gives a good fit. A plot (Fig. 1) of q_t versus t for the fractal-like mixed 1, 2-order model shows that the trend curve is different depending on the adsorbent and can be expressed as parametric model with a growth curve followed exponential pattern within a specific range. The kinetics of AgNPs adsorption on GB, AIOMP, FPC, PFC or AP with an energetically heterogeneous surface determine the adsorption capacity and breakthrough time of the adsorbent of being characterized by its different surface chemical properties (Fayaz et al., 2017; Haerifar and Azizian, 2014). The statistical analysis of experimental data for the adsorption of AgNPs on GB, AIOMP, PFC and AP can be performed using the fractal-like pseudo-first-order, fractal-like exponential, fractal-like pseudo-second-order and mixed 1, 2-order models except for: (1) the use of mixed 1, 2-order model for modeling the adsorption of AgNPs on GB and PFC by using the R^2 , RMSE and MAPE values and AP by using the E_{min} and MAPE values and (2) the use of fractal-like pseudo-second-order model for modeling the adsorption of AgNPs on AP. This conclusion would be due to the use of these models to rank the values of arithmetic mean can provide a good fit within the data range as judged by their AR values of $3.75 \leq AR \leq 7.50$. Previous studies have found the kinetics of AgNPs adsorption on GB, AIOMP, FPC and PFC followed a pseudo-second-order model (Polowczyk et al., 2015; Wu et al., 2017; Zhang et al., 2017; Zhou et al., 2017). It has been reported that the kinetics of adsorption of AgNPs on AP fitted best to pseudo-first-order (Khan et al., 2012). In this work, the use of pseudo-second-order, Boyd, power, exponential, pseudo-first-order, Bangham, Avrami and intraparticle diffusion models can be recommended for modeling the experimental data but it needs to be checked the reliability and validity on a case-by-case basis because of the error analysis of using the different statistical methods for determining the values of R^2 , RMSE, E_{max} , E_{min} , MAPE and MAD can have many reasons for coming to different conclusions of very good, good, satisfactory and poor fit to the experimental data. Experimental evidence (see Tables 3, 5, 7, 9, 11, 13 in Supplementary materials) shows that based on the verification of arithmetic mean as a statistical measure the use of first-order and second-order models cannot be recommended for modeling the experimental data except the use of first order model for modeling the adsorption of AgNPs on FPC due to its statistical data analysis gives a poor fit to the data as judged by an AR value of higher than 11.25. In summary, comprehensive performance analysis of the fifteen kinetic models can rank that the use of the fractal-like mixed 1, 2-order for describing the behaviors of adsorption of AgNPs is better than fractal-like pseudo-first-order,

better than fractal-like exponential, better than fractal-like pseudo-second-order, better than mixed 1, 2-order, better than pseudo-second-order, better than Boyd, better than Power, better than exponential, better than pseudo-first-order, better than Bangham, better than Avrami, better than intraparticle diffusion, better than first order, and better than second-order model as it can be verified by the overall average AR values of 1.61, 3.99, 4.66, 6.05, 7.00, 7.65, 7.94, 8.41, 8.51, 8.63, 8.98, 9.35, 10.70, 12.18, and 14.33, respectively (see Table 13 in Supplementary materials).

3.2.2. Application of the adsorption isotherm models

The error analysis may classify the ranking of the arithmetic mean in term of accuracy for the application of fifteen adsorption isotherm models. The results (Tables 4, 6, 8, 10, 12 in Supplementary materials) show that the use of the isotherm models for modeling the adsorption of AgNPs do fit to the experimental data depending on the type of adsorbent. Even though the experimental evidence of using (1) the Fritz-Schlunder, Baudu and Khan models for modeling the adsorption of AgNPs on GB, (2) the Brouers-Sotolongo model for the adsorption of AgNPs on AIOMP, (3) the Koble-Corrigan and Toth models for the adsorption of AgNPs on FPC, (4) the Freundlich model for the adsorption of AgNPs on PFC and (5) the Maczewski-Jaroniec, Brouers-Sotolongo, Fritz-Schlunder and Baudu models for the adsorption of AgNPs on AP shows a very good fit to the experimental data as judged by the AR value of below 3.75, the statistical analysis of ranking the arithmetic mean verified that no one model can be considered as the most reliable estimate of adsorption isotherm parameters for the adsorption of AgNPs on all adsorbents of GB, AIOMP, FPC, PFC and AP. It has been reported that the experimental data best fitted the Langmuir model for the adsorption of AgNPs on GB, AIOMP, FPC and AP (Khan et al., 2012; Polowczyk et al., 2015; Wu et al., 2017; Zhou et al., 2017). Both Langmuir and Freundlich models fitted the experimental data well for the adsorption of AgNPs on PFC (Zhang et al., 2017). This study found that the most reliable way of analysing the experimental data for the adsorption of AgNPs on GB, AIOMP, PFC and AP can be suggested using the Fritz-Schlunder and Baudu models because of the use of these two models to rank the values of arithmetic mean can give a good fit to the data as judged by the AR values of $3.75 \leq AR \leq 7.50$. The trend curve is different depending on the adsorbent and this can be verified by plotting a curve of q_t versus t as shown in Fig. 2 for the application of Fritz-Schlunder model to describe the behaviours of AgNPs adsorption. This study of the adsorption of AgNPs on GB, AIOMP, FPC, PFC or AP evaluated by the fifteen isotherm models involves plotting the experimental data and finding the different behavior accumulation curves and this suggests that the physical and chemical properties of the adsorbent determine the adsorption capacity and concentration of AgNPs at equilibrium (Adane et al., 2015; Azeez et al., 2018). The application of Fritz-Schlunder, Brouers-Sotolongo, Baudu, Koble-Corrigan, Toth, Maczewski-Jaroniec, Khan, Langmuir-Freundlich, Hill, Radke-Prausnitz, Jovanovic and Unilin models can be recommended for modeling the experimental data since the AR values of less than 11.25 were verified in many cases; however, the verification of the reliability and validity of each model is important for any experimental data to provide guidance and clarity on the specific case of adsorption isotherm because of the error analysis of determining the values of R^2 , RMSE, E_{max} , E_{min} , MAPE and MAD can reach different conclusions of very good, good, satisfactory and poor fit to the experimental data. The experimental evidence of arithmetic mean verification (see Tables 4, 6, 8, 10, 12, 14 in Supplementary materials) shows that the use of Redlich-Peterson model cannot be recommended for modeling the adsorption of AgNPs on AIOMP, FPC, PFC and AP due to the statistical data analysis gives a poor fit to the experimental data as judged by the AR values of higher than

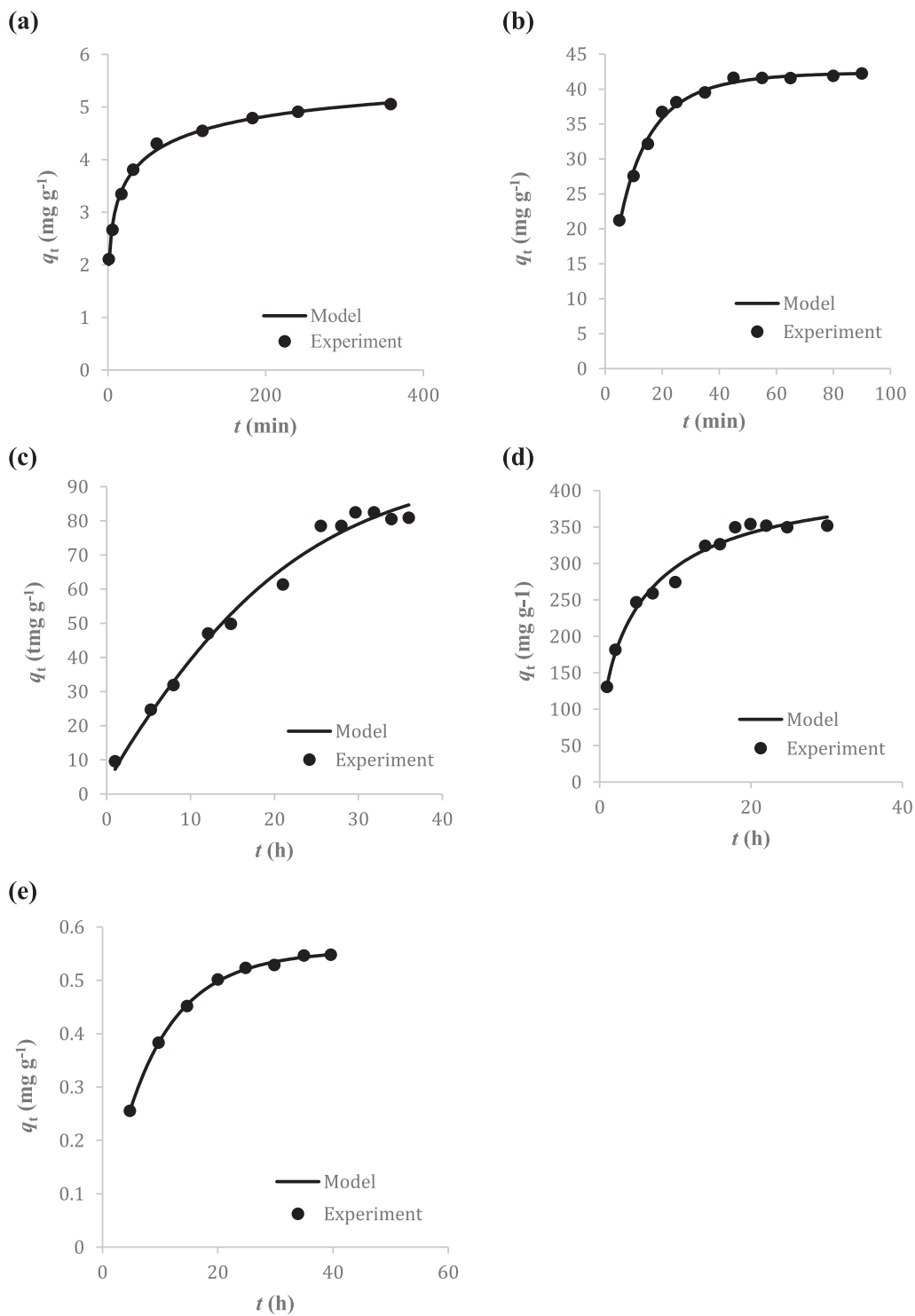


Fig. 1. Curve of plotting q_t versus t for assessing the behaviors of AgNPs adsorption on (a) GB, (b) AlOMP, (c) FPC, (d) PFC and (e) AP by the fractal-like mixed 1, 2-order kinetic model.

11.25. In general, the statistical analysis of the experimental data to evaluate the performance ranking of the fifteen isotherm models may conclude the Fritz-Schlunder better than Brouers-Sotolongo, better than Baudu, better than Koble-Corrigan, better than Toth, better than Maczewski-Jaroniec, better than Khan, better than Langmuir-Freudlich, better than Hill, better than Radke-Prausnitz,

better than Jovanovic, better than Unilin, better than Langmuir, better than Freundlich, and better than Redlich-Peterson as it can be verified by the overall average AR values of 4.17, 4.54, 4.87, 6.27, 6.30, 6.50, 6.60, 7.43, 8.43, 8.57, 9.73, 10.33, 11.37, 11.63, and 12.63, respectively (see Table 14 in Supplementary materials).

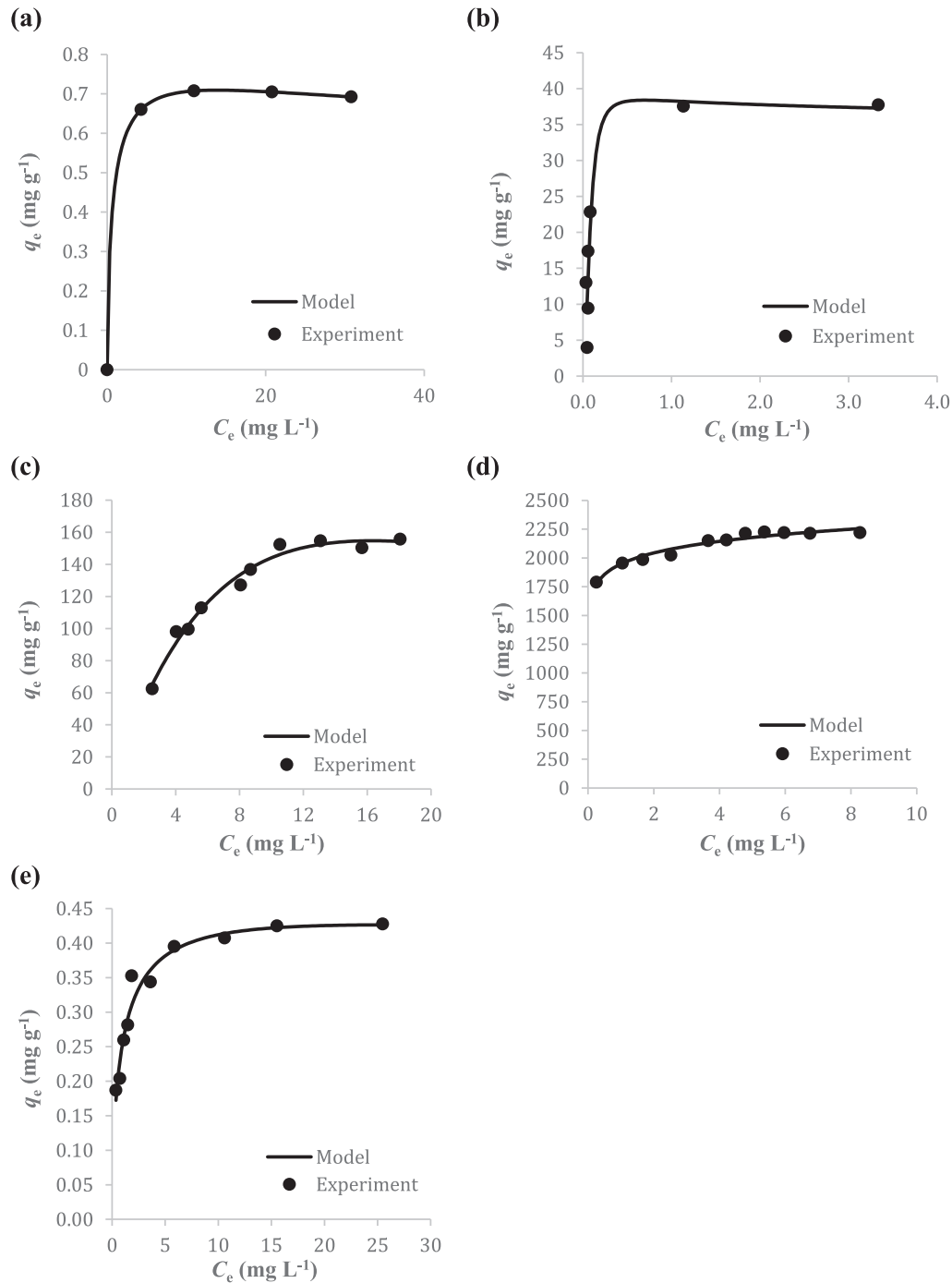


Fig. 2. Curve of plotting q_e versus C_s for assessing the behaviors of AgNPs adsorption on (a) GB, (b) AIOMP, (c) FPC, (d) PFC and (e) AP by the Fritz-Schlunder isotherm model.

4. Conclusions

This study used fifteen kinetic models and fifteen isotherm models together with six statistical analysis methods to assess the level of accuracy for the adsorption of AgNPs from aqueous solution onto the five types of adsorbent. The results of this study verified that the fractal-like mixed 1, 2-order model is the best one among the fifteen kinetic models to be used for describing the behaviors of adsorption of AgNPs on GB, AIOMP, FPC, PFC and AP and the Fritz-Schlunder and Baudu models are the most reliable isotherm models

to be used for describing the behaviors of adsorption of AgNPs on GB, AIOMP, PFC and AP. The verification of the reliability and validity of the match of these thirty models with experimental data would be important to provide guidance and clarity on the kinetic and isotherm studies of AgNPs adsorption on the GB, AIOMP, FPC, PFC and AP adsorbent. The application of other kinetic and isotherm models for studying the adsorption of AgNPs as well as the application of these thirty models for the adsorption of other nanoparticles onto different types of adsorbent would be interested in conducting researches in the future.

Conflict of interest

The authors declare that they have no conflict of interest.

Acknowledgements

The authors thank the financial supports from the Ministry of Higher Education of Malaysia for Research Grant No. R/J130000.7809.4F619, the Universiti Teknologi Malaysia for Research Grant No. Q/J130000.2522.14H40 and the Ministry of Research, Technology and Higher Education of the Republic of Indonesia for Research Grant with the scheme of Penelitian Terapan Unggulan Perguruan Tinggi for the year 2018.

Appendix A. Supplementary data

Supplementary data related to this article can be found at <https://doi.org/10.1016/j.jenvman.2018.03.066>.

References

- Adane, B., Siraj, K., Meka, N., 2015. Kinetic, equilibrium and thermodynamic study of 2-chlorophenol adsorption onto *Ricinus communis* pericarp activated carbon from aqueous solutions. *Green Chem. Lett. Rev.* 8, 3–4, 1–12.
- Ayawei, N., Ebelegi, A.N., Wankasi, D., 2017. Modelling and interpretation of adsorption isotherms. *J. Chem.* 2017, 3039817.
- Azeez, L., Lateef, A., Adebisi, S.A., Oyediji, A.O., 2018. Novel biosynthesized silver nanoparticles from cobweb as adsorbent for Rhodamine B: equilibrium isotherm, kinetic and thermodynamic studies. *Appl. Water Sci.* 8, 32.
- Chen, C., 2003. Evaluation of equilibrium sorption isotherm equations. *Open Chem. Eng. J.* 7, 24–44.
- Chen, Z., Yang, P., Yuan, Z., Guo, J., 2017. Aerobic condition enhances bacteriostatic effects of silver nanoparticles in aquatic environment: an antimicrobial study on *Pseudomonas aeruginosa*. *Sci. Rep.* 7, 7398.
- Cheung, C.W., Porter, J.F., McKay, G., 2001. Sorption kinetic analysis for the removal of cadmium ions from effluents using bone char. *Water Res.* 35, 605–612.
- Conde-González, J.E., Peña-Méndez, E.M., Rybáková, S., Pasán, J., Ruiz-Pérez, C., Havel, J., 2016. Adsorption of silver nanoparticles from aqueous solution on copper-based metal organic frameworks (HKUST-1). *Chemosphere* 150, 659–666.
- Desireddy, A., Conn, B.E., Guo, J., Yoon, B., Barnett, R.N., Monahan, B.M., Kirschbaum, K., Griffith, W.P., Whetten, R.L., Landman, U., Bigioni, T.P., 2013. Ultrastable silver nanoparticles. *Nature* 501, 399–402.
- Fayaz, M., Zarifi, M.H., Abdolrazzagh, M., Shariaty, P., Hashisho, Z., Daneshmand, M., 2017. A novel technique for determining the adsorption capacity and breakthrough time of adsorbents using a noncontact high-resolution microwave resonator sensor. *Environ. Sci. Technol.* 51, 427–435.
- Freundlich, H., 1906. Over the adsorption in solution. *J. Phys. Chem.* 57, 1100–1107.
- Fritz, W., Schluender, E.U., 1974. Simultaneous adsorption equilibria of organic solutes in dilute aqueous solutions on activated carbon. *Chem. Eng. Sci.* 29, 1279–1282.
- Fulazzaky, M.A., 2011. Determining the resistance of mass transfer for adsorption of the surfactant onto granular activated carbons from hydrodynamic column. *Chem. Eng. J.* 166, 832–840.
- Fulazzaky, M.A., 2012. Analysis of global and sequential mass transfers for the adsorption of atrazine and simazine onto granular activated carbons from hydrodynamic column. *Anal. Methods* 4, 2396–2403.
- Fulazzaky, M.A., Khamidun, M.H., Omar, R., 2013. Understanding of mass transfer resistance for the adsorption of solute onto porous material from the modified mass transfer factor models. *Chem. Eng. J.* 228, 1023–1029.
- Fulazzaky, M.A., Khamidun, M.H., Din, M.F.M., Yusoff, A.R.M., 2014. Adsorption of phosphate from domestic wastewater treatment plant effluent onto the laterites in a hydrodynamic column. *Chem. Eng. J.* 258, 10–17.
- Fulazzaky, M.A., Majidnia, Z., Idris, A., 2017. Mass transfer kinetics of Cd(II) ions adsorption by titania polyvinylalcohol-alginate beads from aqueous solution. *Chem. Eng. J.* 308, 700–709.
- Gicheva, G., Yordanov, G., 2013. Removal of citrate-coated silver nanoparticles from aqueous dispersions by using activated carbon. *Coll. Surf. A Physicochem. Eng. Asp.* 431, 51–59.
- Gupta, V.K., Gupta, M., Sharma, S., 2001. Process development for the removal of lead and chromium from aqueous solutions using red mud - an aluminium industry waste. *Water Res.* 35, 1125–1134.
- Haerifar, M., Azizian, S., 2013. An exponential kinetic model for adsorption at solid/solution interface. *Chem. Eng. J.* 215, 65–71.
- Haerifar, M., Azizian, S., 2014. Fractal-like kinetics for adsorption on heterogeneous solid surfaces. *J. Phys. Chem.* 118, 1129–1134.
- Hameed, B.H., Tan, I.A.W., Ahmad, A.L., 2008. Adsorption isotherm, kinetic modeling and mechanism of 2,4,6-trichlorophenol on coconut husk-based activated carbon. *Chem. Eng. J.* 144, 235–244.
- Hill, A.V., 1910. The possible effects of the aggregation of the molecules of haemoglobin on its dissociation curves. *J. Physiol.* 40, 4–7.
- Ho, Y.S., McKay, G., 1998a. A comparison of chemisorption kinetic models applied to pollutant removal on various sorbents. *Process Saf. Environ. Prot.* 76, 332–340.
- Ho, Y.S., McKay, G., 1998b. Sorption of dye from aqueous solution by peat. *Chem. Eng. J.* 70, 115–124.
- Jeppu, G.P., Clement, T.P., 2012. A modified Langmuir-Freundlich isotherm model for simulating pH-dependent adsorption effects. *J. Contam. Hydrol.* 129, 46–53.
- Khambhaty, Y., Mody, K., Basha, S., Jha, B., 2009. Kinetics, equilibrium and thermodynamic studies on biosorption of hexavalent chromium by dead fungal biomass of marine *Aspergillus Niger*. *Chem. Eng. J.* 145, 489–495.
- Khan, A.R., Al-Bahri, T.A., Al-Haddad, A., 1997. Adsorption of phenol based organic pollutants on activated carbon from multicomponent dilute aqueous solutions. *Water Res.* 31, 2102–2112.
- Khan, S.S., Mukherjee, A., Chandrasekaran, N., 2012. Adsorptive removal of silver nanoparticles (SNPs) from aqueous solution by *Aeromonas punctata* and its adsorption isotherm and kinetics. *Coll. Surf. B Biointerf.* 92, 156–160.
- Koble, R.A., Corrigan, T.E., 1952. Adsorption isotherms for pure hydrocarbons. *Ind. Eng. Chem.* 44, 383–387.
- Kumar, A., Vemula, P.K., Ajayan, P.M., John, G., 2008. Silver-nanoparticle-embedded antimicrobial paints based on vegetable oil. *Nat. Mater.* 7, 236–241.
- Kumar, P.S., Senthamarai, C., Durgadevi, A., 2014. Adsorption kinetics, mechanism, isotherm, and thermodynamic analysis of copper ions onto the surface modified agricultural waste. *Environ. Prog. Sustain. Energy* 33, 28–37.
- Lagergren, S., 1898. About the theory of so-called adsorption of soluble substances. *K. Sven. Vetenskapsakademiens Handl.* 24, 1–39.
- Langmuir, I., 1918. The adsorption of gases on plane surfaces of glass, mica and platinum. *J. Am. Chem. Soc.* 40, 1361–1403.
- Le Ouay, B., Stellacci, F., 2015. Antibacterial activity of silver nanoparticles: a surface science insight. *Nano Today* 10, 339–354.
- Lopes, E.C.N., dos Anjos, F.S.C., Vieira, E.F.S., Cestari, A.R., 2003. An alternative Avrami equation to evaluate kinetic parameters of the interaction of Hg(II) with thin chitosan membranes. *J. Coll. Interf. Sci.* 263, 542–547.
- Madhavan, D.B., Kitching, M., Mendham, D.S., Weston, C.J., Baker, T.G., 2016. Mid-infrared spectroscopy for rapid assessment of soil properties after land use change from pastures to *Eucalyptus globulus* plantations. *J. Environ. Manag.* 175, 67–75.
- Marczewski, A.W., 2010. Application of mixed order rate equations to adsorption of methylene blue on mesoporous carbons. *Appl. Surf. Sci.* 256, 5145–5152.
- Matias, M.S., Melegari, S.P., Vicentini, D.S., Matias, W.G., Ricordel, C., Hauchard, D., 2015. Synthetic wastewaters treatment by electrocoagulation to remove silver nanoparticles produced by different routes. *J. Environ. Manag.* 159, 147–157.
- McKay, G., Mesdaghinia, A., Nasser, S., Hadi, M., Aminabad, M.S., 2014. Optimum isotherms of dyes sorption by activated carbon: fractional theoretical capacity and error analysis. *Chem. Eng. J.* 251, 236–247.
- Naik, R.R., Stringer, S.J., Agarwal, G., Jones, S.E., Stone, M.O., 2002. Biomimetic synthesis and patterning of silver nanoparticles. *Nat. Mater.* 1, 169–172.
- Park, M., Im, J., Shin, M., Min, Y., Park, J., Cho, H., Park, S., Shim, M.-B., Jeon, S., Chung, D.-Y., Bae, J., Park, J., Jeong, U., Kim, K., 2012. Highly stretchable electric circuits from a composite material of silver nanoparticles and elastomeric fibres. *Nat. Nanotechnol.* 7, 803–809.
- Plazinski, W., Rudzinski, W., 2009. Kinetics of adsorption at solid/solution interfaces controlled by intraparticle diffusion: a theoretical analysis. *J. Phys. Chem.* 113, 12495–12501.
- Podder, M.S., Majumder, C.B., 2016. Sequestering of As(III) and As(V) from wastewater using a novel neem leaves/MnFe2O4 composite biosorbent. *Int. J. Phytoremed.* 18, 1237–1257.
- Polowczyk, I., Koźlecki, T., Bastrzyk, A., 2015. Adsorption of silver nanoparticles on glass beads surface. *Ads. Sci. Technol.* 33, 731–737.
- Quadros, M.E., Marr, L.C., 2010. Environmental and human health risks of aerosolized silver nanoparticles. *J. Air Waste Manag. Assoc.* 60, 770–781.
- Radke, C.J., Prausnitz, J.M., 1972. Adsorption of organic solutes from dilute aqueous solution of activated carbon. *Ind. Eng. Chem. Fundam.* 11, 445–451.
- Rania, F., Yousef, N.S., 2015. Equilibrium and kinetics studies of adsorption of copper (II) on natural biosorbent. *Int. J. Chem. Eng. Appl.* 6, 319–324.
- Rodríguez, A., García, J., Ovejero, G., Mestanza, M., 2009. Adsorption of anionic and cationic dyes on activated carbon from aqueous solutions: equilibrium and kinetics. *J. Hazard. Mater.* 172, 1311–1320.
- Royer, B., Cardoso, N.F., Lima, E.C., Vaghetti, J.C.P., Simon, N.M., Calvete, T., Veses, R.C., 2009. Applications of Brazilian pine-fruit shell in natural and carbonized forms as adsorbents to removal of methylene blue from aqueous solutions - kinetic and equilibrium study. *J. Hazard. Mater.* 164, 1213–1222.
- Ruiz-Baltazar, A., Reyes-López, S.Y., Tellez-Vasquez, O., Esparza, R., Rosas, G., Pérez, R., 2015. Analysis for the sorption kinetics of Ag nanoparticles on natural clinoptilolite. *Adv. Cond. Matter Phys.* 2015, 284518.
- Shahbeig, H., Bagheri, N., Ghorbanian, S.A., Hallajisani, A., Poorkarimi, S., 2013. A new adsorption isotherm model of aqueous solutions on granular activated carbon. *World J. Model. Simul.* 9, 243–254.
- Sheng, Z., Liu, Y., 2017. Potential impacts of silver nanoparticles on bacteria in the aquatic environment. *J. Environ. Manag.* 191, 290–296.
- Silva, S.M., Sampaio, K.A., Ceriani, R., Verbé, R., Stevens, C., De Greyt, W., Meirelles, A.J.A., 2013. Adsorption of carotenes and phosphorus from palm oil onto acid activated bleaching earth: equilibrium, kinetics and thermodynamics. *J. Food Eng.* 118, 341–349.

- Sivarajasekar, N., Baskar, R., 2014. Adsorption of basic red 9 onto activated carbon derived from immature cotton seeds: isotherm studies and error analysis. *Desalin. Water Treat.* 52, 7743–7765.
- Tripathi, D.K., Tripathi, A., Shweta, Singh, S., Singh, Y., Vishwakarma, K., Yadav, G., Sharma, S., Singh, V.K., Mishra, R.K., Upadhyay, R.G., Dubey, N.K., Lee, Y., Chauhan, D.K., 2017. Uptake, accumulation and toxicity of silver nanoparticle in autotrophic plants, and heterotrophic microbes: a concentric review. *Front. Microbiol.* 8, 07.
- Valenzuela, D.P., Myers, A.L., 1989. *Adsorption Equilibria Data Handbook*. Prentice-Hall, New Jersey.
- Viegas, R.M., Campinas, M., Costa, H., Rosa, M.J., 2014. How do the HSDM and Boyd's model compare for estimating intraparticle diffusion coefficients in adsorption processes. *Adsorption* 20, 737–746.
- Wang, S., Boyjoo, Y., Choueib, A., Zhu, Z.H., 2005. Removal of dyes from aqueous solution using fly ash and red mud. *Water Res.* 39, 129–138.
- Wu, M., Li, Y., Yue, R., Zhang, X., Huang, Y., 2017. Removal of silver nanoparticles by mussel-inspired Fe₃O₄@ polydopamine core-shell microspheres and its use as efficient catalyst for methylene blue reduction. *Sci. Rep.* 7, 42773.
- Zarei, A.R., Barghak, F., 2015. Fast and efficient adsorption of Ag nanoparticles by sodium montmorillonite nanoclay from aqueous systems. *J. Chem. Res.* 39, 542–545.
- Zhang, X.-F., Liu, Z.-G., Shen, W., Gurunathan, S., 2016. Silver nanoparticles: synthesis, characterization, properties, applications, and therapeutic approaches. *Int. J. Mol. Sci.* 17, 1534.
- Zhang, X., Zhang, Y., Zhang, X., Li, S., Huang, Y., 2017. Nitrogen rich core-shell magnetic mesoporous silica as an effective adsorbent for removal of silver nanoparticles from water. *J. Hazard. Mater.* 337, 1–9.
- Zhou, X.-x., Li, Y.-j., Liu, J.-f., 2017. Highly efficient removal of silver-containing nanoparticles in waters by aged iron oxide magnetic particles. *ACS Sustain. Chem. Eng.* 5, 5468–5476.